Molecular Cell

Article

A phage-encoded anti-activator inhibits quorum sensing in *Pseudomonas aeruginosa*

Graphical Abstract

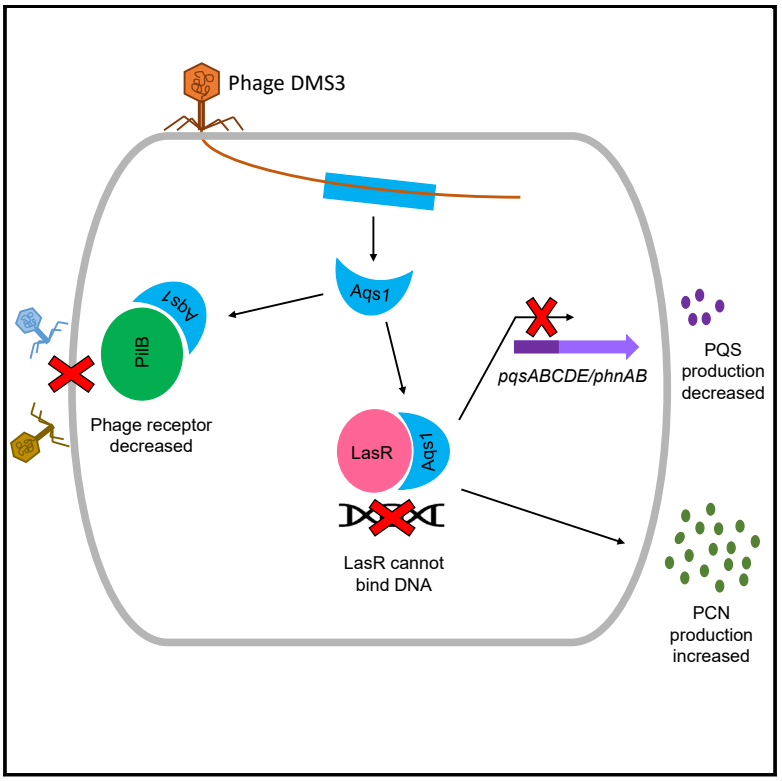

Authors

Megha Shah, Véronique L. Taylor, Diane Bona, ..., Alan R. Davidson, Trevor F. Moraes, Karen L. Maxwell

Correspondence

trevor.moraes@utoronto.ca (T.F.M.), karen.maxwell@utoronto.ca (K.L.M.)

In Brief

Bacteria control expression of anti-phage defenses through a process known as quorum sensing. In this work, Shah et al. characterize a phage protein that inhibits LasR, the master regulator of quorum sensing. This protein provides a counter-defense through which phages might simultaneously silence multiple anti-phage defenses.

Highlights

- Quorum sensing regulates several anti-phage defenses in *Pseudomonas aeruginosa*
- Phage DMS3 encodes a quorum-sensing anti-activator protein that inhibits LasR
- This protein also binds PilB, blocking pilus assembly and further phage infection
- The inhibition of LasR may simultaneously silence multiple anti-phage defenses

Shah et al., 2021, Molecular Cell *81*, 1–13
February 4, 2021
https://doi.org/10.1016/j.molcel.2020.12.011

CellPress

Please cite this article in press as: Shah et al., A phage-encoded anti-activator inhibits quorum sensing in *Pseudomonas aeruginosa*, Molecular Cell (2020), https://doi.org/10.1016/j.molcel.2020.12.011

Molecular Cell

CellPress

Article

A phage-encoded anti-activator inhibits quorum sensing in *Pseudomonas aeruginosa*

Megha Shah,[1,5] Véronique L. Taylor,[1,5] Diane Bona,[1] Yvonne Tsao,[1] Sabrina Y. Stanley,[2] Sheila M. Pimentel-Elardo,[1] Matthew McCallum,[1,3] Joseph Bondy-Denomy,[4] P. Lynne Howell,[1,3] Justin R. Nodwell,[1] Alan R. Davidson,[1,2] Trevor F. Moraes,[1,*] and Karen L. Maxwell[1,6,*]

[1]Department of Biochemistry, University of Toronto, MaRS West Tower, 661 University Avenue, Toronto, ON M5G 1M1, Canada
[2]Department of Molecular Genetics, University of Toronto, MaRS West Tower, 661 University Avenue, Toronto, ON M5G 1M1, Canada
[3]Program in Molecular Structure & Function, Peter Gilgan Centre for Research and Learning, The Hospital for Sick Children, Toronto, ON M5G 0A4, Canada
[4]Department of Microbiology and Immunology, University of California, San Francisco, San Francisco, CA 94143, USA
[5]These authors contributed equally
[6]Lead contact
*Correspondence: trevor.moraes@utoronto.ca (T.F.M.), karen.maxwell@utoronto.ca (K.L.M.)
https://doi.org/10.1016/j.molcel.2020.12.011

SUMMARY

The arms race between bacteria and phages has led to the evolution of diverse anti-phage defenses, several of which are controlled by quorum-sensing pathways. In this work, we characterize a quorum-sensing anti-activator protein, Aqs1, found in *Pseudomonas* phage DMS3. We show that Aqs1 inhibits LasR, the master regulator of quorum sensing, and present the crystal structure of the Aqs1-LasR complex. The 69-residue Aqs1 protein also inhibits PilB, the type IV pilus assembly ATPase protein, which blocks superinfection by phages that require the pilus for infection. This study highlights the remarkable ability of small phage proteins to bind multiple host proteins and disrupt key biological pathways. As quorum sensing influences various anti-phage defenses, Aqs1 provides a mechanism by which infecting phages might simultaneously dampen multiple defenses. Because quorum-sensing systems are broadly distributed across bacteria, this mechanism of phage counter-defense may play an important role in phage-host evolutionary dynamics.

INTRODUCTION

Bacteria use a cell-cell communication system, known as quorum sensing, to collectively control group behaviors in a cell-density-dependent manner (Fuqua et al., 1994). Quorum sensing relies on the production, release, and group-wide detection of diffusible signaling molecules known as autoinducers, with the accumulation of autoinducers at high cell density triggering the activation of genes in a coordinated manner. These systems have been implicated in the battle for survival between bacteria and the phages that infect and kill them. Because the risk of phage infection is greatest at high cell density, the control of costly anti-phage defenses via quorum sensing provides an evolutionary advantage. Accordingly, quorum-sensing systems have been associated with the regulation of anti-phage defense systems. For example, quorum sensing has been shown to upregulate the CRISPR-Cas adaptive immune system in *Pseudomonas aeruginosa* and *Serratia* sp. (Høyland-Kroghsbo et al., 2017; Patterson et al., 2016), downregulate phage receptors on the cell surface in *Vibrio cholerae* and *Escherichia coli* (Hoque et al., 2016; Høyland-Kroghsbo et al., 2013), and increase production of hemagglutinin protease, which inactivates phage particles, in *V. cholerae* (Hoque et al., 2016).

Given the demonstrated role of quorum-sensing systems in mediating anti-phage defenses, in this work, we have investigated the means by which a phage can counter the action of quorum-sensing systems in the Gram-negative bacterium, *P. aeruginosa*. In this opportunistic human pathogen, four quorum-sensing systems have been characterized: the Las and Rhl systems that utilize acylated homoserine lactone signaling molecules (Pesci et al., 1997); the *Pseudomonas* quinolone system (PQS) that uses 2-alkyl-4-quinolones; and the integrated quorum-sensing system (IQS) that relies on 2-(2-hydroxyphenyl)-thiazole-4-carbaldehyde (Lee et al., 2013). These systems are hierarchically arranged, with the Las system at the top of the signaling hierarchy (Figure 1A). LasR acts as a master regulator that activates expression of Rhl and PQS, which additionally regulate each other (Cabeen, 2014; Fuqua et al., 1994; Juhas et al., 2005). In keeping with this hierarchy, inactivation of LasR severely attenuates quorum sensing and the production of quorum-regulated factors.

Several recent lines of evidence imply that quorum-sensing pathways are upregulated upon phage infection in *P. aeruginosa*. For example, it was shown that PQS precursors and metabolites increase in abundance inside phage-infected cells (De Smet et al., 2016), and infection of *P. aeruginosa* by four different phages

Please cite this article in press as: Shah et al., A phage-encoded anti-activator inhibits quorum sensing in *Pseudomonas aeruginosa*, Molecular Cell (2020), https://doi.org/10.1016/j.molcel.2020.12.011

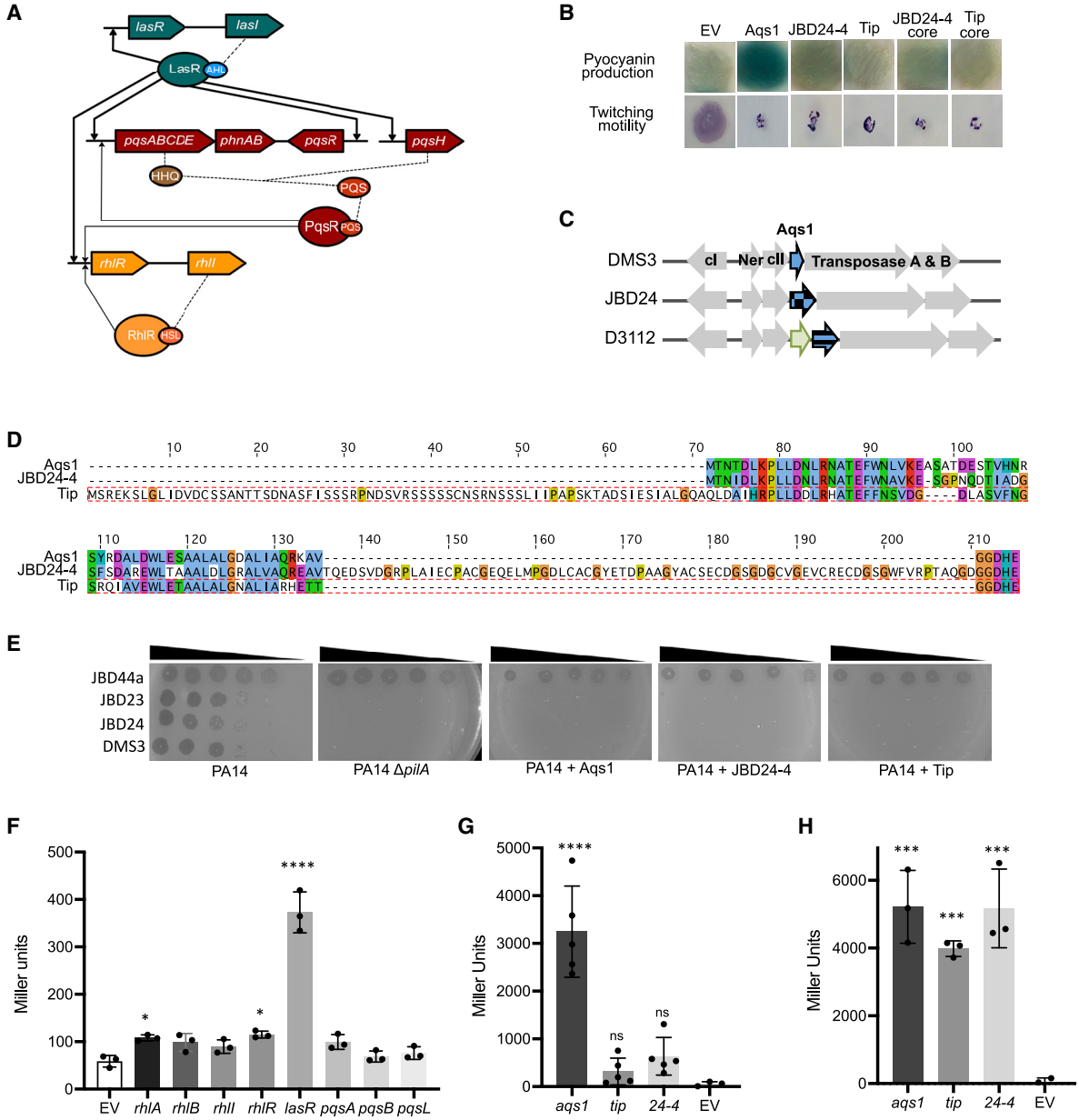

Figure 1. Aqs1 increases pyocyanin production and inhibits twitching motility through interactions with LasR and PilB

(A) Regulatory connections between quorum-sensing pathways in *P. aeruginosa*.

(B) Pyocyanin production and twitching motility of PA14 expressing Aqs1, JBD24-4, Tip, and the core regions of JBD24-4 and Tip that are conserved with Aqs1. EV is empty vector.

(C) The genomic context of Aqs1 and its homologs from phages JBD24 and D3112, each denoted by a blue arrow. Conserved genes cI, cII, Ner, and transposase A and B are in gray. The light green arrow in D3112 designates a hypothetical gene.

(D) Multiple sequence alignment of Aqs1 homologs. Residues are colored by Clustal X format in Jalview. Complete alignment is in Figure S1.

(E) 10-fold dilutions of lipopolysaccharide (LPS)-dependent phage JBD44a and pilus-dependent phages JBD23, JBD24, and DMS3.

(F) Quantification of β-galactosidase activity in the BACTH assay of *aqs1* with quorum-sensing genes.

(G) BACTH β-galactosidase activity showing Aqs1, but not Tip and JBD24-4, interact with LasR.

(H) BACTH β-galactosidase activity showing interaction of Aqs1, Tip, and 24-4 with PilB.

(F)–(H) show mean and standard deviation of three independent replicates. ****$p < 0.0001$, ***$p < 0.001$, *$p < 0.05$, and ns ($p > 0.05$) by one-way ANOVA using Dunnett's test when compared to EV.

Please cite this article in press as: Shah et al., A phage-encoded anti-activator inhibits quorum sensing in *Pseudomonas aeruginosa*, Molecular Cell (2020), https://doi.org/10.1016/j.molcel.2020.12.011

was shown to upregulate transcription of the *pqsABCDE* and *phnAB* operons (Blasdel et al., 2018), both of which are required for the synthesis of the PQS signal (Gallagher et al., 2002; Palmer et al., 2013). Additionally, a PQS-proficient strain of *P. aeruginosa* was shown to evolve higher levels of resistance to phages during a short-term selection experiment (Moreau et al., 2017). Together, these data show that this quorum-sensing system is activated by phage infection and suggest that *P. aeruginosa* may use PQS-mediated quorum sensing to warn surrounding cells of the potential danger of phage invasion. In turn, this could activate expression of the quorum-controlled anti-phage defenses and increase phage resistance in the bacterial community.

Here, we identify and characterize a novel quorum-sensing anti-activator protein encoded by the temperate *P. aeruginosa* phage DMS3. This protein, which we named Aqs1 (anti-quorum-sensing protein 1), inhibits quorum sensing through a direct interaction with the DNA-binding domain of LasR, the master regulator of quorum sensing. Expression of Aqs1 affects a variety of quorum-mediated processes, including pyocyanin production, swarming motility, and protease and rhamnolipid production. Remarkably, Aqs1 also binds PilB, blocking type IV pilus assembly, which is the cell surface receptor for phage DMS3 and many other *P. aeruginosa* phages. We show that deletion of *aqs1* from phage DMS3 leads to increased PQS production during phage infection, illustrating that it impacts quorum signaling and causes a significant alteration in the replicative cycle of the mutant phage. To our knowledge, this is the first phage gene shown to encode an anti-activator protein that modulates bacterial quorum sensing. This work provides important insight into the complex phage-host evolutionary dynamics and reveals a mechanism by which phages could simultaneously inhibit the upregulation of multiple diverse anti-phage defenses.

RESULTS

Aqs1 increases pyocyanin production and inhibits twitching motility

In a previous study, we investigated the biological activities of 14 non-conserved genes (also known as moron genes) from *P. aeruginosa* phages by expressing them individually from a high copy number plasmid (Tsao et al., 2018). We found that expression of most of these genes caused a marked alteration in cellular behavior with respect to motility, virulence factor production, or phage resistance. Continuing along this line of inquiry, we subsequently discovered that expression of another non-conserved phage gene triggered a striking overproduction of pyocyanin, the blue-green pigment that acts as the terminal-signaling molecule in the quorum-sensing pathway (Figures 1B and S2A). This gene, found in phage DMS3 (locus tag DMS3-3, referred to here as *aqs1*), encodes a 69-residue protein. Homologs of *aqs1* are encoded in other *P. aeruginosa* phages closely related to phage DMS3, which are all members of the transposable MP22-like phage family (Bondy-Denomy et al., 2016). In particular, the homolog found in *P. aeruginosa* phage D3112, known as Tip (twitching inhibitory protein), was previously characterized and shown to inhibit twitching motility in *P. aeruginosa* by blocking the activity of PilB, the bacterial ATPase required for type IV pilus assembly (Chung et al., 2014). Another homolog encoded in *P. aeruginosa* phage JBD24 (JBD24-4) was also shown to inhibit twitching motility (Tsao et al., 2018). The genes encoding Aqs1, Tip, and JBD24-4 share a common genomic position between the phage repressor and transposase genes at the left end of the genome, suggesting a shared function (Figure 1C).

Alignment of the Aqs1 protein sequence with its two homologs showed that it shares 72% sequence identity with the N-terminal region of the 143-residue JBD24-4 protein and 49% sequence identity with the C-terminal region of the 136-residue Tip protein (Figure 1D). Tip and JBD24-4 appear to be multi-domain proteins, with each possessing one domain that encompasses the entire 69-residue Aqs1 sequence. We refer to this shared domain as the "core" domain of these proteins. As shown in Figure 1B, plasmid-based expression of Aqs1, Tip, JBD24-4, or the core domains of Tip and JBD24-4 caused a complete loss of twitching motility. Consistent with this loss of twitching motility and in agreement with a previous study that examined Tip and JBD24-4 (Chung et al., 2014; Tsao et al., 2018), expression of Aqs1 and its two homologs also blocked the replication of phages that use type IV pilus as a receptor (Figure 1E). By contrast, replication of phage JBD44a, which uses lipopolysaccharide as its cell surface receptor, was not blocked (Figure 1E). Despite the ability of all three Aqs1 homologs to block type IV pilus function (Figures 1B and S2B), only Aqs1 expression led to pyocyanin overproduction (Figures 1B and S2A).

Aqs1 interacts with the quorum-sensing regulator LasR and the pilus assembly protein PilB

To gain insight into the mechanism of activity of Aqs1 and determine its cellular targets, we used a bacterial adenylate cyclase two-hybrid (BACTH) assay (Karimova et al., 1998) to detect interactions between Aqs1 and its potential protein-binding partners. Because overexpression of Aqs1 resulted in increased pyocyanin production and the synthesis of pyocyanin is primarily controlled through quorum-sensing pathways (Dietrich et al., 2006), we first cloned eight genes known to play roles in this process into a BACTH plasmid. In this assay, interaction between the bait protein (Aqs1) and prey proteins is detected through production of β-galactosidase activity. We found that only expression of LasR, the master regulatory protein of quorum sensing, in combination with Aqs1 resulted in a high level of β-galactosidase activity (Figure 1F) and development of a red color in bacterial colonies grown on MacConkey media (Figure S2C), suggesting that Aqs1 interacts with LasR. Neither Tip nor JBD24-4 showed evidence of interaction with LasR in the BACTH assay (Figure 1G).

Because Aqs1, Tip, and JBD24-4 all inhibit type IV pilus function and Tip was previously shown to interact with PilB (Chung et al., 2014), a protein required for pilus assembly, we also used the BACTH assay to investigate the interaction of these proteins with PilB. We found that Aqs1 and both of its homologs interacted with PilB in this assay (Figure 1H). These experiments imply that Aqs1, Tip, and JBD24-4 all impair type IV pilus function by binding PilB. However, only Aqs1 interacts with LasR, suggesting that the pyocyanin overproduction resulting from Aqs1 expression is mediated through its interaction with LasR.

Please cite this article in press as: Shah et al., A phage-encoded anti-activator inhibits quorum sensing in *Pseudomonas aeruginosa*, Molecular Cell (2020), https://doi.org/10.1016/j.molcel.2020.12.011

Further evidence to connect Aqs1 to LasR was provided by comparing the phenotypes conferred by expression of Aqs1 with those observed in a *P. aeruginosa* strain bearing a deletion of *lasR* (*ΔlasR*). Previous studies have shown that *lasR* mutants overproduce pyocyanin at late stationary phase in cells grown on solid medium and are delayed for pyocyanin production in liquid medium (Dekimpe and Déziel, 2009; Déziel et al., 2005; Diggle et al., 2007). They also display a phenotype known as autolysis when grown on solid medium (D'Argenio et al., 2007) and have decreased levels of extracellular proteases (Van Delden et al., 1998), rhamnolipids (Pearson et al., 1997), and swarming motility (Köhler et al., 2000). We found that cells containing the plasmid expressing Aqs1 display a similar phenotype as the *ΔlasR* mutant in each of these assays (Figures S2D–S2I). Thus, Aqs1 plasmid overexpression provides very similar phenotypes as a *ΔlasR* mutant, suggesting that it is acting as a LasR anti-activator.

Aqs1 is robustly transcribed at the onset of phage infection

The interaction of Aqs1 with LasR led us to hypothesize that it mediates resistance to quorum-controlled anti-phage defenses. If this were true, Aqs1 activity would presumably be required rapidly after the initiation of phage infection. The genomic position of the *aqs1* gene upstream of the gene encoding transposase A (Figure 1C), which is required for the first intracellular step in the life cycle of transposable phages like DMS3 (Marrs and Howe, 1990), suggested that it would be expressed soon after phage DNA injection. To determine when *aqs1* is transcribed, we mixed *P. aeruginosa* strain PA14 cells with phage DMS3 and removed samples at time points up to 1 h following phage addition. We extracted RNA from these samples and quantified the level of *aqs1* transcripts using qRT-PCR. We detected expression of *aqs1* transcript 10 min post-infection (Figure 2A). The level of transcription was approximately equal to that observed for the transposase A gene (*A*), confirming that *aqs1* is an early expressed gene. Transcripts of gene *G*, which is required for assembly of the viral particle and is known to be expressed late in the infection cycle (Stanley et al., 2019), did not accumulate until 60 min post-infection (Figure 2A). The timing of Aqs1 expression is similar to that previously observed for anti-CRISPR proteins that allow phages carrying them to overcome CRISPR-Cas adaptive immunity (Stanley et al., 2019). These results show that *aqs1* transcription is turned on quickly following infection, making it capable of rapidly inhibiting the activities of LasR and/or PilB.

Cells infected by a DMS3 mutant lacking Aqs1 display alterations in growth and quorum sensing

To investigate the impact of Aqs1 on phage fitness, we created a 177-bp in-frame gene deletion in the *aqs1* gene. Because *aqs1* is not conserved among all phages similar to DMS3, we did not expect it to be essential for replication. Consistent with this, we observed no differences in viral particle formation between wild-type DMS3 and DMS3 lacking *aqs1* (DMS3$^{\Delta aqs1}$). For example, equal numbers of phage particles were spontaneously produced from cultures of wild-type and DMS3$^{\Delta aqs1}$ lysogens that were diluted 1:100 and grown for 6 h in rich medium (Figure 2B). In addition, the number of phages produced following mitomycin induction of the wild-type or mutant lysogens and spontaneous production during overnight growth were also equal (Figure 2C). We further examined the effects of *aqs1* deletion on twitching motility and phage resistance in a DSM3 lysogen. We found that there was no difference in the twitching zones when comparing DMS3 and DMS3$^{\Delta aqs1}$ lysogens (Figure 2D). The DMS3$^{\Delta aqs1}$ lysogen also maintained resistance to phage infection, although slight zones of growth inhibition where high titers of phages were spotted suggest that Aqs1 does provide some level of protection against superinfection (Figure 2E). These results can be explained by our prior finding that phage DMS3 encodes other superinfection exclusion proteins that are expressed from the lysogen (e.g., gp61) that function to inhibit twitching motility and confer phage resistance (Tsao et al., 2018).

Given that Aqs1 expression impinges on quorum sensing, we reasoned that the effect of *aqs1* deletion might only manifest at a particular stage of the cellular growth cycle. To address this, we mixed cells at low density with varying initial phage concentrations (i.e., varying multiplicity of infection [MOI]) and monitored cell growth. In these experiments, the optical density of the culture increases for several hours as bacterial replication outstrips phage replication. However, at a certain time point, phage replication overwhelms cellular growth and the optical density of the culture drops sharply as the bulk of cells are lysed by the action of replicating phages (Figure 2F). The time point at which this lysis event occurs depends on the MOI, with lysis occurring sooner at high multiplicity (Figure S3A). After the lysis event, cell density increases again. As DMS3 is a temperate phage, the cells growing at this point are mostly lysogens, which are resistant to further infection, or phage-resistant mutants. When the growth profiles of cells infected with wild-type DMS3 and DMS3$^{\Delta aqs1}$ were compared in this experiment, a highly reproducible difference was observed. At all multiplicities of infection tested, DMS3$^{\Delta aqs1}$ exhibited a much steeper drop in optical density at the lysis event, and the cell density decreased to a considerably greater extent (Figures 2F and S3A). This implies that fewer cells survive infection by DMS3$^{\Delta aqs1}$.

To gain further insight into the role of Aqs1, we repeated the growth cycle assays at an MOI of 1 and monitored the viable cell numbers and phage plaque-forming units present in the culture at various times. We found that the number of viable cells in the cultures infected by wild-type DMS3 and DMS3$^{\Delta aqs1}$ were similar up to 5 h post-infection (Figure 2G). In subsequent time points, the lysis event occurred and the viable cell numbers in the culture infected by DMS3$^{\Delta aqs1}$ decreased markedly relative to the number in the culture infected by wild-type DMS3, reaching a maximum at the 6.5- and 7-h time points, where approximately 100-fold fewer viable cells were present in the DMS3$^{\Delta aqs1}$ infection (Figure 2G). Despite the difference in the number of viable cells present after the lysis event, more phages were not produced by the DMS3$^{\Delta aqs1}$ phage cultures between 3 and 7 h (Figure 2H).

To ascertain how many of the cells surviving after the lysis event were protected from subsequent infection by prophage formation, we determined the number of lysogenic cells present in the DMS3- and DMS3$^{\Delta aqs1}$-infected cultures. We screened 50 cells from each culture at time points between 3 and 7 h and

Please cite this article in press as: Shah et al., A phage-encoded anti-activator inhibits quorum sensing in *Pseudomonas aeruginosa*, Molecular Cell (2020), https://doi.org/10.1016/j.molcel.2020.12.011

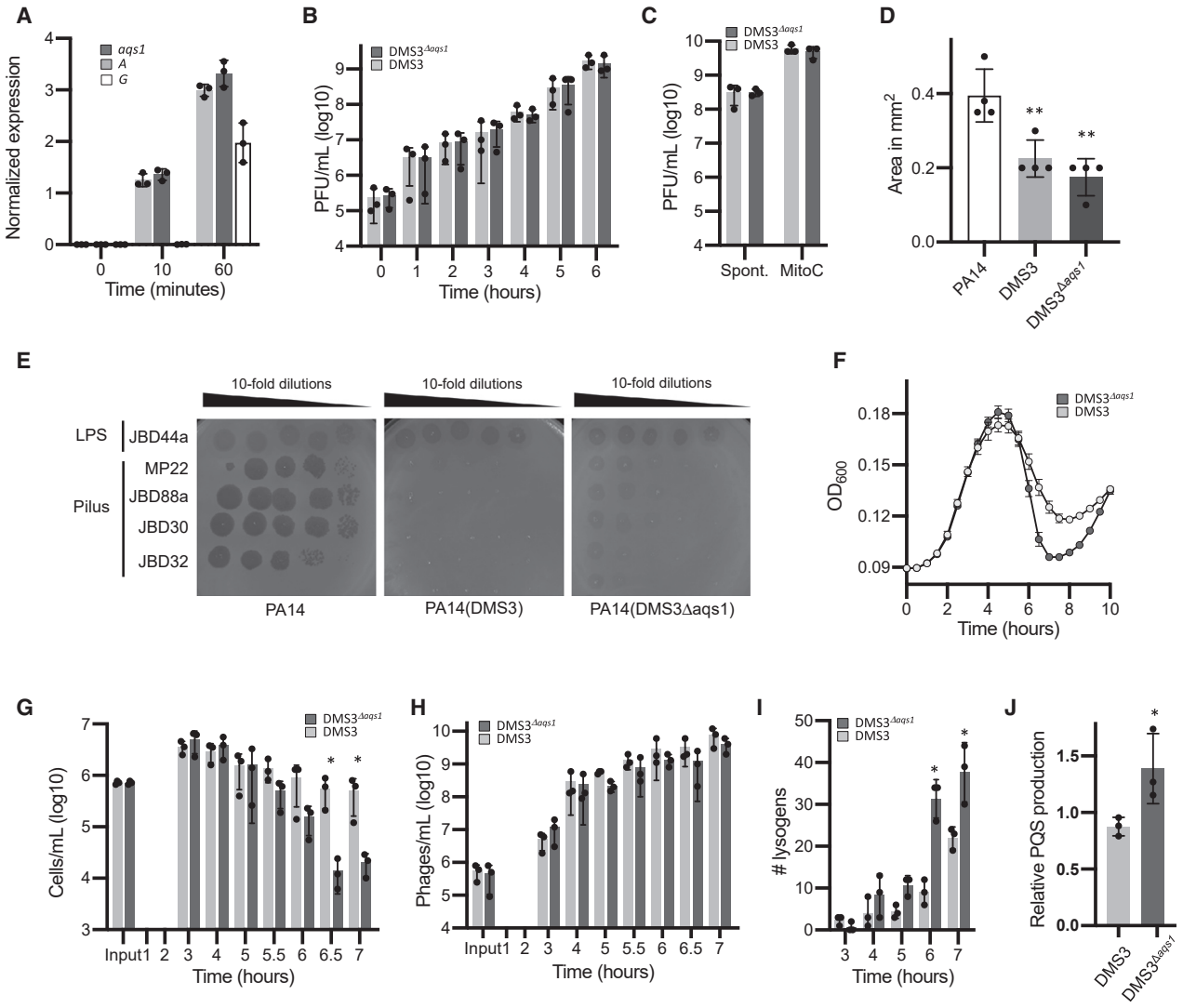

Figure 2. Aqs1 is expressed early in phage infection and promotes cell lysis

(A) Relative transcription levels of phage genes measured by qRT-PCR at the indicated time points after infection with DMS3vir. Transcription levels are shown for *aqs1* (dark gray), *A* (light gray), and *G* (white).

(B) Spontaneous production of phage particles from lysogens of wild-type DMS3 and DMS3$^{\Delta aqs1}$.

(C) Phage production from lysogens of wild-type DMS3 and DMS3$^{\Delta aqs1}$ spontaneously produced during overnight growth (spont.) and in the presence of mitomycin C (MitoC). Three biological replicates plotted as mean ± SD (A–C)

(D) Twitching motility of lysogens of DMS3 and DMS3$^{\Delta aqs1}$ in PA14. Four biological replicates plotted as mean ± SD, **$p < 0.01$ by one-way ANOVA when compared to wild-type PA14.

(E) Phage resistance profiles: 10-fold serial dilutions of JBD44a (LPS dependent) and MP22, JBD88a, JBD30, and JBD32 (type IV pilus dependent) plated on wild-type PA14 and lysogens of DMS3 and DMS3$^{\Delta aqs1}$ in PA14.

(F) Growth curves of PA14 infected with DMS3 and DMS3$^{\Delta aqs1}$ at an MOI of 1.

(G) Number of live bacterial cells present at various time points between 1 and 7 h for the experiment shown in (F). DMS3 and DMS3$^{\Delta aqs1}$ cell counts shown are the average of three biological replicates, with standard deviations.

(H) Phage production for the infection experiments shown in (F) for DMS3 and DMS3$^{\Delta aqs1}$.

(I) Number of lysogens in cultures infected by DMS3 and DMS3$^{\Delta aqs1}$ (shown in F).

(J) PQS production 5 h post-infection in cultures challenged with DMS3 (light gray) and DMS3 $^{\Delta aqs1}$ (dark gray).

Three biological replicates plotted as mean ± SD (G, I, and J) *$p < 0.05$ by paired t test.

discovered that the number of lysogens in each culture was approximately equal up until 5 h (Figure 2I). At 6 h, corresponding to the lysis event, we found that approximately 15% of the viable cells in the wild-type DMS3 infection were lysogens. By contrast, about 75% of the surviving cells in the DMS3$^{\Delta aqs1}$ infection were lysogens. Given that there are 100-fold fewer overall viable cells present in the DMS3$^{\Delta aqs1}$-infected cells, we conclude that the lack of Aqs1 is leading to increased cell death during the

Please cite this article in press as: Shah et al., A phage-encoded anti-activator inhibits quorum sensing in *Pseudomonas aeruginosa*, Molecular Cell (2020), https://doi.org/10.1016/j.molcel.2020.12.011

infection process and that lysogens are more capable of surviving under these conditions. This may be due to an abortive infection response, whereby cells sense the invading phage and commit altruistic suicide. The net outcome of this response is that cells do not survive the infection but prevent the propagation and release of phage progeny (Chopin et al., 2005). Alternatively, the increased cell death could be a result of loss of superinfection exclusion activity, a phenomenon in which the activity of a phage protein prevents a secondary infection with the same or a closely related phage (Abedon, 2015; Chopin et al., 2005). In the case of Aqs1, expression could result in rapid disruption of pilus formation through its interaction with PilB, the pilus assembly ATPase. As DMS3 uses the pilus as a cell surface receptor, the PilB-binding activity of Aqs1 could prevent a single cell from being infected by multiple DMS3 phages. Thus, loss of Aqs1 activity in the DMS3$^{\Delta aqs1}$ mutant could potentially allow multiple phages to infect in rapid succession. This, in turn, might allow them to overcome host anti-phage defenses and lead to increased cell death.

Because Aqs1 appears to inhibit the quorum-sensing regulator LasR, we sought to identify a direct output of the quorum-sensing system that varied during infection by phages lacking *aqs1*. To this end, we used mass spectrometry to assess the levels of PQS, a quorum-sensing molecule that was previously shown to be induced upon phage infection (De Smet et al., 2016). Strikingly, cultures of cells infected with DMS3$^{\Delta aqs1}$ showed a 30% increase in PQS levels in the media compared to an uninfected PA14 culture 5 h after infection, just before the concerted cell lysis event (Figure 2J). By contrast, media from the culture infected with wild-type DMS3 contained slightly less PQS than the uninfected cells. These data suggest that the activity of Aqs1 modulates the production of at least one relevant quorum-sensing controlled molecule. Although PQS levels were markedly elevated during infection by DMS3$^{\Delta aqs1}$, the growth profiles of wild-type DMS3- and DMS3$^{\Delta aqs1}$-infected cultures still displayed the same noticeable difference when these phages were grown on PA14 mutants in genes *pqsA* and *pqsH*, which do not produce PQS (Figures S3A–S3C). Thus, although the growth difference observed when the DMS3$^{\Delta aqs1}$ mutant infects PA14 is not mediated directly through the PQS pathway, these data do show that Aqs1 expression impinges on production of a quorum-sensing molecule. As LasR activity is known to positively regulate PQS production, we postulate that Aqs1 binding to LasR inhibits the upregulation of the PQS pathway during wild-type DMS3 infection, although the DMS3$^{\Delta aqs1}$ mutant is unable to keep this system silenced.

The Aqs1 structure reveals an interaction with the DNA-binding domain of LasR

To gain insight into how Aqs1 modulates pyocyanin production and twitching motility, we solved its three-dimensional structure using X-ray crystallography. We determined the structure of Aqs1 to a resolution of 2.0 Å in space group $P3_12$ 1 (Table 1; PDB: 6V7U) and found that it forms a dimeric α-helical bundle (Figure 3A), with each monomer composed of two α helices separated by a short loop sequence. The dimeric structure is consistent with the native molecular weight of this protein in solution as estimated by size exclusion chromatography followed by multi-angle light scattering (SEC-MALS) (Figure S4C). We also solved the structure in a second space group, *C*2, to a resolution of 2.3 Å using molecular replacement (Table 1; PDB: 6V7V). To better understand the mechanism by which Aqs1 inhibits LasR activity, we also determined its structure bound to full-length LasR. The Aqs1-LasR complex crystallized in two different space groups, $P2_12_12_1$ and $P4_12_12$. The structures were determined to a resolution of 3.0 Å (PDB: 6V7W) and 2.9 Å (PDB: 6V7X), respectively, by molecular replacement using our apo Aqs1 structure and a previously determined LasR ligand binding domain structure (PDB: 3IX3) as starting models. Statistics of the structure determination and refinement are summarized in Table 1.

The Aqs1-LasR co-crystal structure revealed a dimeric LasR complex in which the DNA-binding domain of each LasR subunit is bound to an Aqs1 dimer (Figure 3B). The N-terminal ligand-binding domain of LasR consists of an α-β-α sandwich with one autoinducer (3-oxo-C_{12}-HSL) buried in a pocket between the central 5-stranded antiparallel β sheet and the adjacent helices as previously observed (Bottomley et al., 2007). The ligand-binding domain of our structure could be overlaid with the previously determined LasR ligand-binding domain structure with a root-mean-square deviation (RMSD) of 0.51 Å over 1,958 atoms (Figure S5A). The DNA binding domain, which encodes a canonical helix-turn-helix motif, is attached to the ligand-binding domain by a short linker sequence. Although no full-length structure of LasR has been previously solved, that of a related quorum-sensing protein from *Agrobacterium tumefaciens* has been determined in complex with a target DNA sequence (Figure S5B). Although it only shares 16% sequence identity with LasR (Bottomley et al., 2007), the *A. tumefaciens* TraR ligand-binding domain monomer closely resembles that in our LasR structure, overlaying with an RMSD of 1.34 Å over 376 backbone atoms. Comparison of the TraR DNA-bound complex with our LasR-Aqs1 structure revealed several important features. First, in the Aqs1-bound structure, overlaying the helix-turn-helix motif of LasR with that of the DNA-bound TraR reveals that Aqs1 binding occurs directly over the DNA-binding interface (Figure 3C). Thus, the interaction of Aqs1 with LasR would be expected to block binding to the major groove of the DNA, such that even N-acyl homoserine lactone (AHL)-bound LasR would be unable to bind the promoters and activate quorum-regulated genes. Second, one monomer in each of the Aqs1 dimers interacts with the N-terminal sequence of each LasR monomer (Figures 3B and S5C). This keeps the DNA-binding domains pinned to opposite sides of the LasR dimer and would further inhibit the ability of the DNA-binding domains to interact with DNA. This constrained mobility of the DNA-binding domains also likely explains the success of structure determination of full-length LasR in the presence of Aqs1.

To confirm that Aqs1 inhibits LasR DNA binding, we performed electrophoretic mobility shift assays (EMSAs) using the *lasB* operator 1 (OP1) site as a target DNA sequence as previously described (Kafle et al., 2016). LasR was purified in the presence of 3-oxo-C_{12}-HSL, and DNA binding was assessed in the absence or presence of Aqs1. As can be seen in Figure 4A, LasR alone binds the OP1 site, resulting in a shift in DNA mobility. When Aqs1 was added to the reaction, LasR is no longer able to bind the OP1 oligonucleotide, as shown by the absence of a

Please cite this article in press as: Shah et al., A phage-encoded anti-activator inhibits quorum sensing in *Pseudomonas aeruginosa*, Molecular Cell (2020), https://doi.org/10.1016/j.molcel.2020.12.011

Table 1. Data collection and refinement statistics

	LasR-Aqs1	LasR-Aqs1	Aqs1	Aqs1
PDB code	6V7X	6V7W	6V7U	6V7V
Phasing method	MR	MR	Se-SAD	MR
Data collection				
Space group	P 4_1 2_1 2	P 2_1 2_1 2_1	P 3_1 2 1	C 1 2 1
a, *b*, *c* (Å)	104.536 104.536 102.601	97.975 100.438 106.631	66.41 66.41 73.3	114.73 66.12 73.21
α, β, γ (°)	90 90 90	90 90 90	90 90 120	90 90.03 90
Wavelength	0.97920	0.97920	0.97944	0.97944
Resolution range	73.22–2.9 (3.004–2.9)	73.11–3.0 (3.107–3.0)	45.247–2.0 (2.080–2.0)	45.17–2.3 (2.347–2.3)
Total reflections	26,230 (2,534)	40,673 (4,250)	24,345 (13,715)	47,309 (9,286)
Multiplicity	2.0 (2.0)	2.0 (2.0)	10.8 (10.6)	3.8 (3.8)
Completeness (%)	99.92 (99.68)	99.90 (99.81)	99.33 (98.39)	99.60 (99.38)
Mean I/sigma (I)	31.89 (2.38)	19.26 (1.38)	13.81 (1.96)	12.07 (3.00)
R-merge	0.01176 (0.3027)	0.02027 (0.3987)	0.1623 (1.726)	0.1404 (0.8981)
R-meas	0.01663 (0.428)	0.02866 (0.5639)	0.1704 (1.813)	0.1633 (1.043)
CC1/2	1 (0.897)	1 (0.791)	0.998 (0.758)	0.995 (0.754)
Refinements				
Reflections used in refinement	13,107 (1,265)	21,666 (2,124)	12,967 (1,287)	24,440 (2,419)
R-work/R-free	0.2491/0.2806	0.2496/0.2717	0.2134/0.2574	0.2053/0.2442
Number of non-hydrogen atoms	2,702	5,480	977	2,837
Macromolecules	2,653	5,427	932	2,737
Ligands	21	42		
Solvent	28	11	45	100
Protein residues	337	689	120	352
RMS (bonds)	0.0037	0.002	0.006	0.006
RMS (angles)	0.70	0.61	0.69	0.79
Ramachandran favored (%)	95.14	94.81	99.12	98.50
Ramachandran outliers (%)	0.00	0.74	0.00	0.00
Rotamer outliers (%)	0.36	0.00	0.00	0.00
Average B-factor	113.8	103.63	42.13	45.50
Macromolecules	113.94	103.80	42.38	45.62
Ligands	92.91	84.50		
Solvent	113.60	91.41	37.08	42.40

Statistics for the highest-resolution shell are shown in parentheses. MR, molecular replacement; SAD, single anomalous diffraction.

change in DNA mobility. These data show that Aqs1 interacts with the LasR DNA-binding domain and prevents LasR from binding a target DNA operator sequence.

Aqs1 uses distinct residues to bind LasR and PilB

Our previous biological assays and BACTH results revealed that Aqs1, but not Tip and JBD24-4, interacted with the LasR transcriptional regulator, although all three interacted with PilB. To identify the regions of the protein that mediate these interactions, we used a combination of structure and sequence comparisons. Aqs1 shares 72% sequence identity with JBD24-4, yet only Aqs1 interacts with LasR and inhibits quorum sensing. We identified regions in which the sequences differed (Figure 4B) and engineered mutants in which the Aqs1 sequence was substituted with the sequence from JBD24-4 ($Aqs1^{GPNQD}$, $Aqs1^{IADG}$, and $Aqs1^{FSDARE}$). We then tested the ability of these mutant proteins to mediate pyocyanin overproduction and twitching inhibition (Figures 4C and 4D). We found that $Aqs1^{FSDARE}$, in which residues Y39-D44 were replaced with residues F38-E43 from JBD24-4, lost the ability to overproduce pyocyanin but maintained the ability to inhibit twitching motility. These results confirm that the protein is still folded and stable as it retains the twitching phenotype. We next determined that $Aqs1^{FSDARE}$ no longer interacted with LasR in the BACTH assay (Figure S7B). These data show that residues Y39-D44 of Aqs1 mediate the interaction with LasR and that this interaction is important for controlling the quorum-sensing phenotype observed. Mapping this mutation back on the LasR-Aqs1 complex structure showed that this region of Aqs1 interacts directly with the recognition domain of the LasR helix-turn-helix motif (Figure 4E). These data confirm the biological significance of the interaction observed in the crystal structure.

To identify residues in Aqs1 that interact with PilB, we compared the sequences of Aqs1, Tip, and JBD24-4 and

Please cite this article in press as: Shah et al., A phage-encoded anti-activator inhibits quorum sensing in *Pseudomonas aeruginosa*, Molecular Cell (2020), https://doi.org/10.1016/j.molcel.2020.12.011

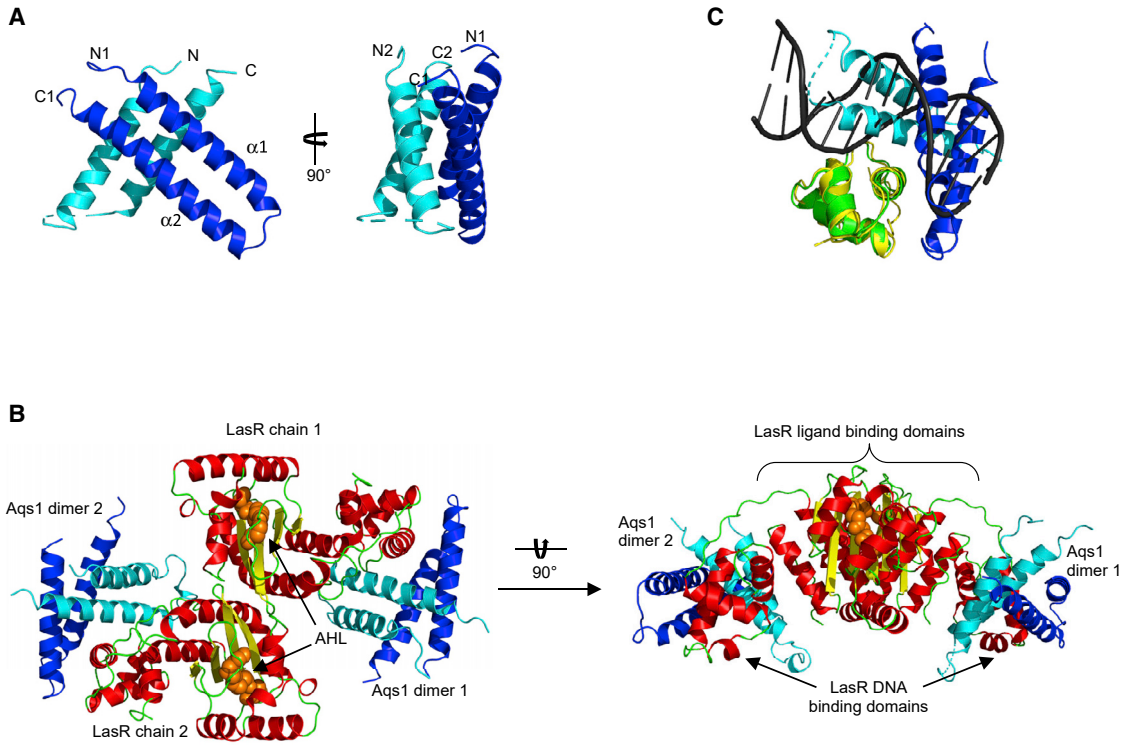

Figure 3. Aqs1 interacts with LasR through the DNA-binding domain

(A) The crystal structure of Aqs1. Monomers are shown in blue and cyan.

(B) The Aqs1-LasR complex reveals an interaction through the DNA-binding domain. Two LasR monomers, each bound to 3-oxo-C_{12}-HSL (AHL), interact through their ligand-binding domains. Aqs1 dimers are shown in blue and cyan.

(C) Overlay of the DNA-binding domains of our LasR structure (PDB: 6V7X; yellow) and the TraR DNA-bound complex (PDB: 1H0M; green). The DNA is shown in black, and Aqs1 bound to LasR DNA-binding domain in blue and cyan (see also Figure S5).

identified five conserved residues (R14, E18, F19, W20, and W45) that were exposed on the surface of the Aqs1 structure. We substituted each of these five positions with alanine and tested their abilities to inhibit twitching motility and interact with PilB in the BACTH assay. We identified two mutants, F19A and W45A, that lost the ability to inhibit twitching motility (Figure 4F) and no longer interacted with PilB in the BACTH assay (Figure S7A). They did, however, still interact with LasR and overproduce pyocyanin (Figures 4G and S7B). These data show that Aqs1 mediates interactions with LasR and PilB through two different binding surfaces (Figure 4E) and that the loss of one interaction does not result in the loss of the other.

Aqs1 homologs with the LasR-interacting residues are distributed across a variety of *Pseudomonas* phages and strains

Although our initial bioinformatic analyses revealed many homologs of Aqs1, our biochemical investigations show non-conserved residues are critical for the interaction with LasR. To determine how common the LasR interaction is, we examined Aqs1 homologs and identified 43 that contained the LasR-interacting motif (Table S1). These homologs are all very similar, encoding proteins of 69 residues with pairwise sequence identities of 97% or more. One exception, found in a clinical isolate of *P. aeruginosa*, encoded the extra C-terminal domain seen in JBD24-4. However, the core region that aligned with Aqs1 shared 97% sequence identity. In cases where we could map the phage genome that the Aqs1 homolog was found in, we found highly similar genomic organizations, with the percent identity to DMS3 across these genomes ranging from 39% to 89% (Table S1). Each of these homologs was found in the same genomic context as Aqs1, between the repressor and transposase genes, suggesting that the activity of this protein is required early in the phage infection cycle.

DISCUSSION

In recent years, a number of diverse anti-phage defenses have been shown to be upregulated by bacterial quorum-sensing systems (Hoque et al., 2016; Høyland-Kroghsbo et al., 2013, 2017; Patterson et al., 2016). This is thought to protect the bacterial community from phage infection at high cell density, when the risk of a phage epidemic is greatest. In this work, we show that *Pseudomonas* phage DMS3 encodes a quorum-sensing anti-activator protein, Aqs1, which is expressed immediately following phage infection. Aqs1 has dual functions; it inhibits the activity of LasR, the master regulator of quorum sensing, and it binds to the type IV pilus assembly ATPase protein, PilB,

Please cite this article in press as: Shah et al., A phage-encoded anti-activator inhibits quorum sensing in *Pseudomonas aeruginosa*, Molecular Cell (2020), https://doi.org/10.1016/j.molcel.2020.12.011

CellPress

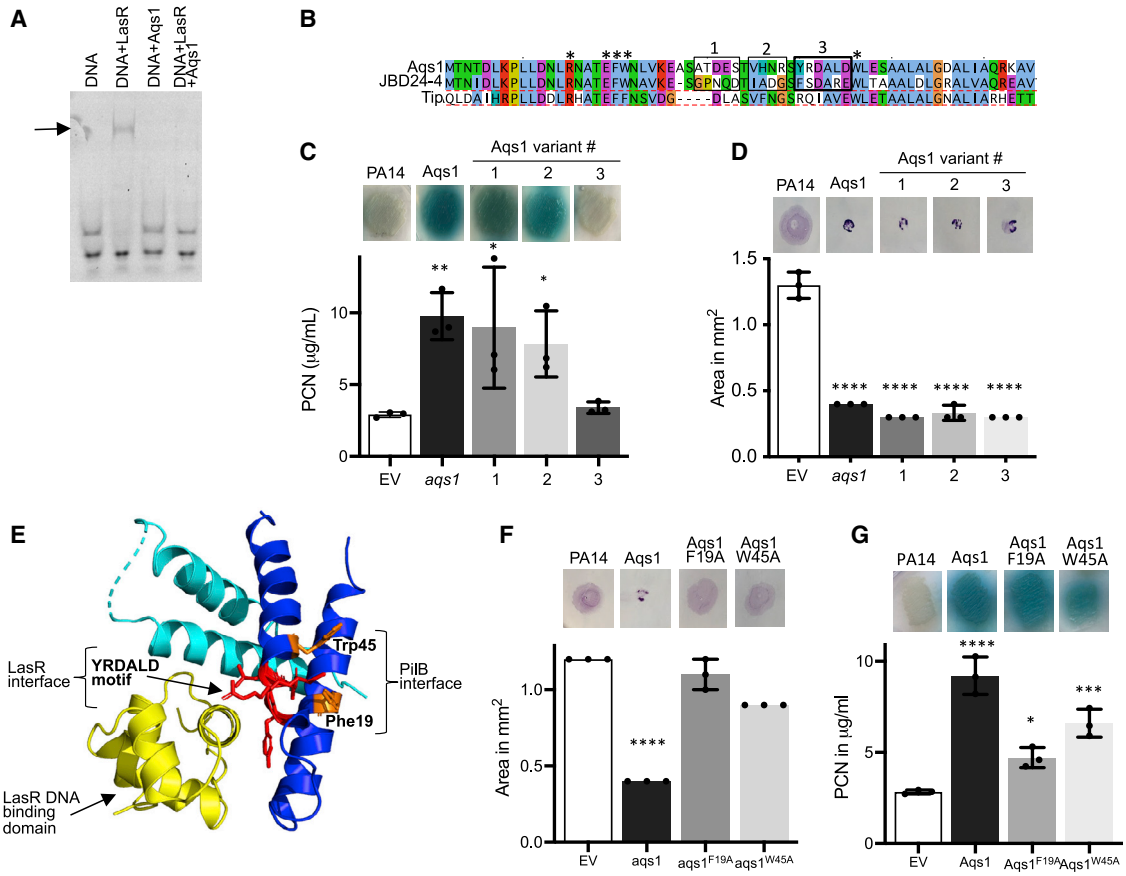

Figure 4. Aqs1 interacts with LasR and PilB through two distinct interfaces

(A) Representative EMSA with a double-stranded DNA fragment containing the *lasB* OP1 site. The arrow indicates the shifted LasR-bound DNA. Protein purification is shown in Figure S6.

(B) Sequence alignment of Aqs1 with core regions of JBD24-4 and Tip. Boxes denote motifs in Aqs1 replaced by sequences from JBD24-4; asterisks designate conserved residues substituted with Ala.

(C) Pyocyanin production from plasmid-expressed Aqs1 and variants 1, 2, and 3 (as in B).

(D) Twitching motility for plasmid-expressed Aqs1 and variants grown overnight in LB agar.

(E) Location of the LasR and PilB interacting residues on the blue monomer of Aqs1. The cyan Aqs1 monomer is behind. The LasR-binding motif YRDALD is colored red; residues F19 and W45 involved in PilB binding are colored orange. The LasR DNA-binding domain is shown in yellow.

(F and G) Representative twitching motility (F) and pyocyanin production (G) assays for F19A and W45A mutants.

(C), (D), (F), and (G) show mean ± SD of three independent replicates. ****$p < 0.0001$, ***$p < 0.001$, **$p < 0.01$, *$p < 0.05$, and ns ($p > 0.05$) by one-way ANOVA when compared to EV.

inhibiting twitching motility and superinfection by pilus-dependent phages. Collectively, these activities endow phages expressing Aqs1 with the potential to block upregulation of quorum-mediated anti-phage defenses and protect infected cells from attack by other phages.

As expected for an anti-activator protein, the biological activities we observed upon constitutive expression of Aqs1 from a plasmid mimic the effects that result from *lasR* deletion, including changes in pyocyanin production, autolysis, and virulence factor production. We also showed that Aqs1 expression from the phage genome during infection restrains production of the quorum-sensing-controlled PQS signaling molecule. This implies an effect on LasR activity, which is known to be required for PQS production (Pesci et al., 1999). Notably, we found that infection by DMS3$^{\Delta aqs1}$ markedly increased production of PQS, which agrees with studies showing that phage infection activates this pathway (Blasdel et al., 2018; De Smet et al., 2016). However, this effect was not elicited by wild-type DMS3, only by the mutant phage that lacked Aqs1. Previous studies showed that infection by only some *P. aeruginosa* phages elicited PQS production and suggested that phages might encode inhibitors that interfere with its production (Blasdel et al., 2018; De Smet et al., 2016). Our results confirm this hypothesis.

Although phage challenge had previously been shown to stimulate systems controlled by quorum sensing (Blasdel et al., 2018; De Smet et al., 2016), the effects of this stimulation on phage-infected cell growth had not previously been measured. Here, by comparing the effects of wild-type DMS3 and DMS3$^{\Delta aqs1}$ infections, we can infer the impact of pathways controlled by LasR. At

Please cite this article in press as: Shah et al., A phage-encoded anti-activator inhibits quorum sensing in *Pseudomonas aeruginosa*, Molecular Cell (2020), https://doi.org/10.1016/j.molcel.2020.12.011

first glance, our observation that infection by DMS3$^{\Delta aqs1}$ results in 100-fold greater cell death than infection by wild-type DMS3 seems paradoxical, as one would expect quorum-sensing activated mechanisms to protect cells from phage attack. However, bacteria often defend themselves against phage attack through abortive infection mechanisms, whereby infected cells die precociously in order to block the production of phages. During infection by DMS3$^{\Delta aqs1}$, quorum-sensing stimulated pathways activated by LasR may be contributing to cell death. These pathways would be suppressed by the action of Aqs1 during a wild-type DMS3 infection. The effect of an anti-phage mechanism is indicated by our observation that more phages are not produced during the DMS3$^{\Delta aqs1}$ infection cycle, even though 100-fold more cells are killed. If this cell death were occurring through normal phage replication, then a much greater yield of phage particles would be expected. Also supporting the action of a quorum-sensing controlled mechanism is the increased level of PQS observed during DMS3$^{\Delta aqs1}$ infection and the manifestation of the difference between wild-type and DMS3$^{\Delta aqs1}$ infection only at a late time point in the infection cycle.

Although PQS production is increased in the absence of Aqs1, the putative anti-phage mechanism affecting the DMS3$^{\Delta aqs1}$ phage does not rely on PQS because the same response occurs in the *pqsA* and *pqsH* mutant bacterial strains that are unable to produce PQS. In this case, the change in PQS level serves as a hallmark of an alteration in quorum sensing, but other quorum-sensing stimulated systems appear to be responsible for the marked difference between cells infected by wild-type DMS3 and DMS3$^{\Delta aqs1}$ phages. It is possible that PQS-mediated anti-phage responses play an important role in different *P. aeruginosa* strains or under different environmental conditions. For example, PQS production in response to phage infection was recently shown to repel healthy *P. aeruginosa* populations growing on solid medium, thereby limiting the spread of phage infection (Bru et al., 2019). Thus, although DMS3$^{\Delta aqs1}$ can still replicate robustly in PA14 under our test conditions, *aqs1* may be critical for DMS3 survival when infecting other *P. aeruginosa* strains in varying environments. This idea is supported by highly variable complement of anti-phage defense systems detected in strains of *P. aeruginosa* (Doron et al., 2018).

In *P. aeruginosa*, other anti-activator proteins that suppress quorum sensing through LasR have been previously characterized; QslA binds the ligand-binding domain of LasR, disrupting dimerization and preventing binding to the promoters of las responsive genes (Fan et al., 2013), and QteE decreases LasR protein stability *in vivo* and prevents its accumulation in the cell (Siehnel et al., 2010). However, Aqs1 is distinct from these other inhibitors in being encoded by a phage and utilizing a different inhibitory mechanism. Inhibition of LasR through a direct interaction with the DNA-binding domain has not previously been observed, and the conformational stabilization of the full-length LasR protein by Aqs1 binding allowed the first structural determination of the complete LasR protein.

A remarkable feature of the 69-residue Aqs1 protein is its ability to target both LasR and PilB, two unrelated proteins that function in completely different biological pathways. This highlights the strong evolutionary pressure on phages to (1) evolve activities to control host functions and (2) economize genome size to one that can fit within the confines of the phage capsid. The interaction of Aqs1 with PilB prevents assembly of pili on the cell surface and provides protection against further phage infection. As assembly and retraction of the pilus is an ongoing process, inhibition of the ATPase motor that promotes assembly should provide tight control of this process. The expression of Aqs1 immediately upon phage infection presumably shuts down pilus assembly quite rapidly and likely serves to limit the number of phages that can infect a single cell. This ability to inhibit phages from entering cells that are already infected may play a role in the differences observed for the growth curves of wild-type DMS3 and DMS3$^{\Delta aqs1}$. This activity of Aqs1 brings to mind the classic superinfection exclusion proteins affecting *E. coli* T-even phages, Sp and Imm, whose activities prevent phage progeny from entering cells that are already infected (Dulbecco, 1952; Emrich, 1968; Vallée and Cornett, 1972). As cells that are already infected are not productive hosts for additional phages that adsorb following the primary infection event, this activity would serve to protect phage progeny from executing non-productive infections. This is thought to be a very important adaptation in environments where there are ample free phages and a scarcity of bacterial hosts (Abedon, 1990, 2019).

The ability of bacterial quorum-sensing systems to coordinate the expression of a variety of different anti-phage responses provides a powerful and generalized weapon that can be used to protect against phage infection. As quorum-sensing systems are broadly distributed across diverse bacteria and have been shown to regulate anti-phage responses in a number of different bacterial species, this mechanism of control is likely widespread. In this study, we demonstrate that *P. aeruginosa* phage DMS3 encodes an inhibitor of quorum sensing that may be used to broadly inhibit these quorum-controlled anti-phage activities through its interaction with LasR. Specialized phage-encoded inhibitors of single bacterial anti-phage defenses, such as anti-CRISPRs (Bondy-Denomy et al., 2013; Pawluk et al., 2016), anti-restriction (Spoerel et al., 1979), and anti-BREX (Isaev et al., 2020) proteins, have been previously described. By contrast, Aqs1 and its homologs provide a new and more global mechanism through which a single phage protein might silence multiple anti-phage defenses simultaneously though the interruption of quorum-sensing pathways. Future studies to determine the precise mechanisms of action of Aqs1 and to characterize other phage-encoded inhibitors of quorum-meditated anti-phage defenses will provide valuable new insight into the phage-host evolutionary arms race.

Limitations

We did not definitively link inhibition of LasR by Aqs1 with phage resistance. These studies are extremely challenging for several reasons. First, the temporary inhibition of LasR that occurs during phage infection is very different from a deletion strain lacking LasR. Although LasR is positioned higher in the quorum-sensing hierarchy, RhlR is able to compensate for its absence in the deletion strain. Also, deletion of LasR results in widespread changes in gene expression, complicating these analyses. Finally, expression from Aqs1 from a plasmid showed much more pronounced phenotypes than expression from the phage, complicating our ability to easily study the effects of mutations in

this protein. The ability of Aqs1 to bind both LasR and PilB also confounds interpretation of the DMS3$^{\Delta aqs1}$ phage effects. We did not show that the mutants had differential effects in the context of the phage or determine whether the ability of Aqs1 to bind two proteins is central to its function. The ability to determine binding constants for Aqs1 with LasR and PilB was hampered by the inherent insolubility of these proteins. It will be important to identify a direct mechanism through which the LasR-binding function of Aqs1 affects quorum-mediated pathways in the context of phage infection and to determine whether the dual binding specificity of this protein is critical for its function.

STAR★METHODS

Detailed methods are provided in the online version of this paper and include the following:

- KEY RESOURCES TABLE
- RESOURCE AVAILABILITY
  - Lead contact
  - Materials availability
  - Data and code availability
- EXPERIMENTAL MODEL AND SUBJECT DETAILS
  - Bacterial strains
  - Phage strains
- METHOD DETAILS
  - DNA cloning and manipulation
  - Pyocyanin production assay
  - Twitching motility assays
  - Protease production assay
  - Rhamnolipid production assay
  - Swarming motility assay
  - Identification of protein interaction partners using the bacterial two-hybrid assay
  - Protein expression and purification
  - Crystallization of Aqs1 alone and LasR-Aqs1 complex
  - Data collection and structure determination
  - Size exclusion chromatography-multi angle light scattering (SEC-MALS)
  - Electrophoretic mobility shift assays (EMSAs)
  - Preparation of P. aeruginosa phages and plaque assays
  - Generating mutants of aqs1 in the DMS3 phage
  - PA14 phage infection assays
  - P. aeruginosa PA14 cell counts and lysogen determination during phage infection
  - Spontaneous phage induction in liquid culture growth measurement
  - PQS quantification during infection with phage DMS3
  - RNA Extraction and RT-qPCR of DMS3 during infection
- QUANTIFICATION AND STATISTICAL ANALYSIS

SUPPLEMENTAL INFORMATION

Supplemental Information can be found online at https://doi.org/10.1016/j.molcel.2020.12.011.

ACKNOWLEDGMENTS

This work was supported by grants from the Canadian Institutes of Health Research to K.L.M. (MOP-136845 andPJT-165936), T.F.M. (PJT-148795), A.R.D. (FDN-15427), and P.L.H. (FDN-154327 and MOP-93585); the Canada Research Chairs program (T.F.M., A.R.D., and P.L.H.); and the Canada Foundation for Innovation (K.L.M. and T.F.M.).

AUTHOR CONTRIBUTIONS

Conceptualization, K.L.M., M.S., and V.L.T.; Methodology, K.L.M., M.S., and V.L.T.; Investigation, M.S., V.L.T., D.B., Y.T., S.Y.S., S.M.P.-E., M.M., and J.B.-D.; Writing – Original Draft, K.L.M., M.S., and V.L.T.; Writing – Review and Editing, S.Y.S., M.M., J.B.-D., P.L.H., J.R.N., A.R.D., T.F.M., and K.L.M.; Visualization, K.L.M., M.S., and V.L.T.; Supervision, P.L.H., J.R.N., A.R.D., T.F.M., and K.L.M.; Funding Acquisition, K.L.M. and T.F.M.

DECLARATION OF INTERESTS

The authors declare no competing interests.

Received: October 26, 2020
Revised: November 19, 2020
Accepted: December 3, 2020
Published: January 6, 2021

REFERENCES

Abedon, S.T. (1990). Selection for lysis inhibition in bacteriophage. J. Theor. Biol. *146*, 501–511.

Abedon, S.T. (2015). Bacteriophage secondary infection. Virol. Sin. *30*, 3–10.

Abedon, S.T. (2019). Look who's talking: T-even phage lysis inhibition, the granddaddy of virus-virus intercellular communication research. Viruses *11*, 951.

Blasdel, B.G., Ceyssens, P.J., Chevallereau, A., Debarbieux, L., and Lavigne, R. (2018). Comparative transcriptomics reveals a conserved bacterial adaptive phage response (BAPR) to viral predation. bioRxiv.

Bondy-Denomy, J., Pawluk, A., Maxwell, K.L., and Davidson, A.R. (2013). Bacteriophage genes that inactivate the CRISPR/Cas bacterial immune system. Nature *493*, 429–432.

Bondy-Denomy, J., Qian, J., Westra, E.R., Buckling, A., Guttman, D.S., Davidson, A.R., and Maxwell, K.L. (2016). Prophages mediate defense against phage infection through diverse mechanisms. ISME J. *10*, 2854–2866.

Bottomley, M.J., Muraglia, E., Bazzo, R., and Carfi, A. (2007). Molecular insights into quorum sensing in the human pathogen Pseudomonas aeruginosa from the structure of the virulence regulator LasR bound to its autoinducer. J. Biol. Chem. *282*, 13592–13600.

Bru, J.L., Rawson, B., Trinh, C., Whiteson, K., Høyland-Kroghsbo, N.M., and Siryaporn, A. (2019). PQS produced by the Pseudomonas aeruginosa stress response repels swarms away from bacteriophage and antibiotics. J. Bacteriol. *201*, e00383-19.

Cabeen, M.T. (2014). Stationary phase-specific virulence factor overproduction by a lasR mutant of Pseudomonas aeruginosa. PLoS ONE *9*, e88743.

Cady, K.C., Bondy-Denomy, J., Heussler, G.E., Davidson, A.R., and O'Toole, G.A. (2012). The CRISPR/Cas adaptive immune system of Pseudomonas aeruginosa mediates resistance to naturally occurring and engineered phages. J. Bacteriol. *194*, 5728–5738.

Chopin, M.C., Chopin, A., and Bidnenko, E. (2005). Phage abortive infection in lactococci: variations on a theme. Curr. Opin. Microbiol. *8*, 473–479.

Chung, I.Y., Jang, H.J., Bae, H.W., and Cho, Y.H. (2014). A phage protein that inhibits the bacterial ATPase required for type IV pilus assembly. Proc. Natl. Acad. Sci. USA *111*, 11503–11508.

D'Argenio, D.A., Wu, M., Hoffman, L.R., Kulasekara, H.D., Déziel, E., Smith, E.E., Nguyen, H., Ernst, R.K., Larson Freeman, T.J., Spencer, D.H., et al.

(2007). Growth phenotypes of Pseudomonas aeruginosa lasR mutants adapted to the airways of cystic fibrosis patients. Mol. Microbiol. *64*, 512–533.

De Smet, J., Zimmermann, M., Kogadeeva, M., Ceyssens, P.J., Vermaelen, W., Blasdel, B., Bin Jang, H., Sauer, U., and Lavigne, R. (2016). High coverage metabolomics analysis reveals phage-specific alterations to Pseudomonas aeruginosa physiology during infection. ISME J. *10*, 1823–1835.

Dekimpe, V., and Déziel, E. (2009). Revisiting the quorum-sensing hierarchy in Pseudomonas aeruginosa: the transcriptional regulator RhlR regulates LasR-specific factors. Microbiology (Reading) *155*, 712–723.

Déziel, E., Gopalan, S., Tampakaki, A.P., Lépine, F., Padfield, K.E., Saucier, M., Xiao, G., and Rahme, L.G. (2005). The contribution of MvfR to Pseudomonas aeruginosa pathogenesis and quorum sensing circuitry regulation: multiple quorum sensing-regulated genes are modulated without affecting lasRI, rhlRI or the production of N-acyl-L-homoserine lactones. Mol. Microbiol. *55*, 998–1014.

Dietrich, L.E., Price-Whelan, A., Petersen, A., Whiteley, M., and Newman, D.K. (2006). The phenazine pyocyanin is a terminal signalling factor in the quorum sensing network of Pseudomonas aeruginosa. Mol. Microbiol. *61*, 1308–1321.

Diggle, S.P., Griffin, A.S., Campbell, G.S., and West, S.A. (2007). Cooperation and conflict in quorum-sensing bacterial populations. Nature *450*, 411–414.

Doron, S., Melamed, S., Ofir, G., Leavitt, A., Lopatina, A., Keren, M., Amitai, G., and Sorek, R. (2018). Systematic discovery of antiphage defense systems in the microbial pangenome. Science *359*, eaar4120.

Dulbecco, R. (1952). Mutual exclusion between related phages. J. Bacteriol. *63*, 209–217.

Emrich, J. (1968). Lysis of T4-infected bacteria in the absence of lysozyme. Virology *35*, 158–165.

Emsley, P., Lohkamp, B., Scott, W.G., and Cowtan, K. (2010). Features and development of Coot. Acta Crystallogr. D Biol. Crystallogr. *66*, 486–501.

Fan, H., Dong, Y., Wu, D., Bowler, M.W., Zhang, L., and Song, H. (2013). QsIA disrupts LasR dimerization in antiactivation of bacterial quorum sensing. Proc. Natl. Acad. Sci. USA *110*, 20765–20770.

Fuqua, W.C., Winans, S.C., and Greenberg, E.P. (1994). Quorum sensing in bacteria: the LuxR-LuxI family of cell density-responsive transcriptional regulators. J. Bacteriol. *176*, 269–275.

Gallagher, L.A., McKnight, S.L., Kuznetsova, M.S., Pesci, E.C., and Manoil, C. (2002). Functions required for extracellular quinolone signaling by Pseudomonas aeruginosa. J. Bacteriol. *184*, 6472–6480.

Goldschmidt, L., Cooper, D.R., Derewenda, Z.S., and Eisenberg, D. (2007). Toward rational protein crystallization: a Web server for the design of crystallizable protein variants. Protein Sci. *16*, 1569–1576.

Ha, D.G., Kuchma, S.L., and O'Toole, G.A. (2014). Plate-based assay for swarming motility in Pseudomonas aeruginosa. Methods Mol. Biol. *1149*, 67–72.

Hoque, M.M., Naser, I.B., Bari, S.M., Zhu, J., Mekalanos, J.J., and Faruque, S.M. (2016). Quorum regulated resistance of Vibrio cholerae against environmental bacteriophages. Sci. Rep. *6*, 37956.

Høyland-Kroghsbo, N.M., Maerkedahl, R.B., and Svenningsen, S.L. (2013). A quorum-sensing-induced bacteriophage defense mechanism. MBio *4*, e00362-12.

Høyland-Kroghsbo, N.M., Paczkowski, J., Mukherjee, S., Broniewski, J., Westra, E., Bondy-Denomy, J., and Bassler, B.L. (2017). Quorum sensing controls the Pseudomonas aeruginosa CRISPR-Cas adaptive immune system. Proc. Natl. Acad. Sci. USA *114*, 131–135.

Isaev, A., Drobiazko, A., Sierro, N., Gordeeva, J., Yosef, I., Qimron, U., Ivanov, N.V., and Severinov, K. (2020). Phage T7 DNA mimic protein Ocr is a potent inhibitor of BREX defence. Nucleic Acids Res. *48*, 5397–5406.

Jeong, J.Y., Yim, H.S., Ryu, J.Y., Lee, H.S., Lee, J.H., Seen, D.S., and Kang, S.G. (2012). One-step sequence- and ligation-independent cloning as a rapid and versatile cloning method for functional genomics studies. Appl. Environ. Microbiol. *78*, 5440–5443.

Juhas, M., Eberl, L., and Tümmler, B. (2005). Quorum sensing: the power of cooperation in the world of Pseudomonas. Environ. Microbiol. *7*, 459–471.

Kabsch, W. (2010). Xds. Acta Crystallogr. D Biol. Crystallogr. *66*, 125–132.

Kafle, P., Amoh, A.N., Reaves, J.M., Suneby, E.G., Tutunjian, K.A., Tyson, R.L., and Schneider, T.L. (2016). Molecular insights into the impact of oxidative stress on the quorum-sensing regulator protein LasR. J. Biol. Chem. *291*, 11776–11786.

Karimova, G., Pidoux, J., Ullmann, A., and Ladant, D. (1998). A bacterial two-hybrid system based on a reconstituted signal transduction pathway. Proc. Natl. Acad. Sci. USA *95*, 5752–5756.

King, M.M., Guragain, M., Sarkisova, S.A., and Patrauchan, M.A. (2016). Pyocyanin extraction and quantitative analysis in swarming *Pseudomonas aeruginosa*. Bio-protocol *6*, e2042.

Köhler, T., Curty, L.K., Barja, F., van Delden, C., and Pechère, J.C. (2000). Swarming of Pseudomonas aeruginosa is dependent on cell-to-cell signaling and requires flagella and pili. J. Bacteriol. *182*, 5990–5996.

Lee, J., Wu, J., Deng, Y., Wang, J., Wang, C., Wang, J., Chang, C., Dong, Y., Williams, P., and Zhang, L.H. (2013). A cell-cell communication signal integrates quorum sensing and stress response. Nat. Chem. Biol. *9*, 339–343.

Liebschner, D., Afonine, P.V., Baker, M.L., Bunkóczi, G., Chen, V.B., Croll, T.I., Hintze, B., Hung, L.W., Jain, S., McCoy, A.J., et al. (2019). Macromolecular structure determination using X-rays, neutrons and electrons: recent developments in Phenix. Acta Crystallogr. D Struct. Biol. *75*, 861–877.

Marrs, C.F., and Howe, M.M. (1990). Kinetics and regulation of transcription of bacteriophage Mu. Virology *174*, 192–203.

McCallum, M., Tammam, S., Little, D.J., Robinson, H., Koo, J., Shah, M., Calmettes, C., Moraes, T.F., Burrows, L.L., and Howell, P.L. (2016). PilN binding modulates the structure and binding partners of the Pseudomonas aeruginosa type IVa pilus protein PilM. J. Biol. Chem. *291*, 11003–11015.

Moreau, P., Diggle, S.P., and Friman, V.P. (2017). Bacterial cell-to-cell signaling promotes the evolution of resistance to parasitic bacteriophages. Ecol. Evol. *7*, 1936–1941.

Palmer, G.C., Jorth, P.A., and Whiteley, M. (2013). The role of two Pseudomonas aeruginosa anthranilate synthases in tryptophan and quorum signal production. Microbiology (Reading) *159*, 959–969.

Patterson, A.G., Jackson, S.A., Taylor, C., Evans, G.B., Salmond, G.P.C., Przybilski, R., Staals, R.H.J., and Fineran, P.C. (2016). Quorum sensing controls adaptive immunity through the regulation of multiple CRISPR-Cas systems. Mol. Cell *64*, 1102–1108.

Pawluk, A., Amrani, N., Zhang, Y., Garcia, B., Hidalgo-Reyes, Y., Lee, J., Edraki, A., Shah, M., Sontheimer, E.J., Maxwell, K.L., et al. (2016). Naturally occurring off-switches for CRISPR-Cas9. Cell *167*, 1829–1838.e9.

Pearson, J.P., Pesci, E.C., and Iglewski, B.H. (1997). Roles of Pseudomonas aeruginosa las and rhl quorum-sensing systems in control of elastase and rhamnolipid biosynthesis genes. J. Bacteriol. *179*, 5756–5767.

Pesci, E.C., Pearson, J.P., Seed, P.C., and Iglewski, B.H. (1997). Regulation of las and rhl quorum sensing in Pseudomonas aeruginosa. J. Bacteriol. *179*, 3127–3132.

Pesci, E.C., Milbank, J.B., Pearson, J.P., McKnight, S., Kende, A.S., Greenberg, E.P., and Iglewski, B.H. (1999). Quinolone signaling in the cell-to-cell communication system of Pseudomonas aeruginosa. Proc. Natl. Acad. Sci. USA *96*, 11229–11234.

Sandoz, K.M., Mitzimberg, S.M., and Schuster, M. (2007). Social cheating in Pseudomonas aeruginosa quorum sensing. Proc. Natl. Acad. Sci. USA *104*, 15876–15881.

Schrodinger (2015). The AxPyMOL molecular graphics plugin for Microsoft PowerPoint, version 1.8 (Schrodinger).

Siehnel, R., Traxler, B., An, D.D., Parsek, M.R., Schaefer, A.L., and Singh, P.K. (2010). A unique regulator controls the activation threshold of quorum-regulated genes in Pseudomonas aeruginosa. Proc. Natl. Acad. Sci. USA *107*, 7916–7921.

Spoerel, N., Herrlich, P., and Bickle, T.A. (1979). A novel bacteriophage defence mechanism: the anti-restriction protein. Nature *278*, 30–34.

Stanley, S.Y., Borges, A.L., Chen, K.H., Swaney, D.L., Krogan, N.J., Bondy-Denomy, J., and Davidson, A.R. (2019). Anti-CRISPR-associated proteins are crucial repressors of anti-CRISPR transcription. Cell *178*, 1452–1464.e13.

Tsao, Y.F., Taylor, V.L., Kala, S., Bondy-Denomy, J., Khan, A.N., Bona, D., Cattoir, V., Lory, S., Davidson, A.R., and Maxwell, K.L. (2018). Phage morons play an important role in Pseudomonas aeruginosa phenotypes. J. Bacteriol. *200*, e00189-18.

Vallée, M., and Cornett, J.B. (1972). A new gene of bacteriophage T4 determining immunity against superinfecting ghosts and phage in T4-infected Escherichia coli. Virology *48*, 777–784.

Van Delden, C., Pesci, E.C., Pearson, J.P., and Iglewski, B.H. (1998). Starvation selection restores elastase and rhamnolipid production in a Pseudomonas aeruginosa quorum-sensing mutant. Infect. Immun. *66*, 4499–4502.

Please cite this article in press as: Shah et al., A phage-encoded anti-activator inhibits quorum sensing in *Pseudomonas aeruginosa*, Molecular Cell (2020), https://doi.org/10.1016/j.molcel.2020.12.011

STAR★METHODS

KEY RESOURCES TABLE

REAGENT or RESOURCE	SOURCE	IDENTIFIER
Bacterial and virus strains		
Pseudomonas aeruginosa strain UCBPP-PA14	K. Maxwell Lab	NC_008463.1
Pseudomonas phage DMS3	K. Maxwell Lab	NC_020198.1
Pseudomonas phage JBD24	A. Davidson Lab	NC_020203
Pseudomonas phage JBD26	A. Davidson Lab	GCA_002601925.1
Pseudomonas phage DMS3vir	A. Davidson Lab	N/A
Pseudomonas phage DMS3$^{\Delta aqs1}$	This paper	N/A
Escherichia coli DH5α	K. Maxwell Lab	N/A
Escherichia coli BL21(DE3)	K. Maxwell Lab	N/A
Escherichia coli BL21(DE3) B834	T. Moraes Lab	N/A
Chemicals, peptides, and recombinant proteins		
Acid phenol:chloroform	Ambion	Cat#AM9722
Ni-NTA agarose resin	QIAGEN	Cat#30210
SYBR Gold nucleic acid stain	Invitrogen	Cat#S11494
3-oxo-C_{12}-HSL	Sigma	Cat#09139
Fluorescein	IDT	6-FAM
Purified protein: Aqs1, LasR	This paper	N/A
Critical commercial assays		
TURBO DNA-free kit	Ambion	Cat#AM1907
SuperScript IV VILO master mix	Invitrogen	Cat#11754050
PowerUp SYBR Green master mix	Applied Biosystems	Cat#A25741
In-Fusion HD cloning kit	Clonetech	Cat#638912
Phusion High-Fidelity DNA Polymerase	Thermo Scientific	Cat#F530S
Deposited data		
Aqs1 crystal structure Se-SAD	This paper	PDB: 6V7U
Aqs1 crystal structure MR	This paper	PDB: 6V7V
LasR-Aqs1 crystal structure MR	This paper	PDB: 6V7W
LasR-Aqs1 crystal structure MR	This paper	PDB: 6V7X
Oligonucleotides		
5′ATCAAGGCTACCTGCCAGTTCTGGCAG GTTTGGCCGCGGGTTC-3′	This paper	lasB OP1 site
Recombinant DNA		
pHERD30T (gent^{R})	A. Davidson Lab	GenBank: EU603326.1
pHERD20T (amp^{R})	A. Davidson Lab	GenBank: EU603324.1
p15TV-L	Addgene	ID #26093
pETDUET	Novagen	ID #71146
pUT18C	P.L. Howell Lab	Euromedex
pKT25	P.L. Howell Lab	Euromedex
Software and algorithms		
Prism 7.0	GraphPad	http://www.graphpad.com/scientific-software/prism
Image Lab 6.0	BioRad	https://www.bio-rad.com/en-ca/product/image-lab-software
PyMol	Schrödinger	https://pymol.org/2/
Jalview	Jalview	http://www.jalview.org
PHENIX suite	PHENIX	https://www.phenix-online.org
Coot	Coot	https://www2.mrc-lmb.cam.ac.uk/personal/pemsley/coot/

Please cite this article in press as: Shah et al., A phage-encoded anti-activator inhibits quorum sensing in *Pseudomonas aeruginosa*, Molecular Cell (2020), https://doi.org/10.1016/j.molcel.2020.12.011

CellPress

RESOURCE AVAILABILITY

Lead contact

Further information and requests for resources and reagents should be directed to and will be fulfilled by the Lead Contact, Karen Maxwell (karen.maxwell@utoronto.ca).

Materials availability

All unique/stable reagents generated in this study are available from the Lead Contact without restriction.

Data and code availability

This study did not generate/analyze datasets or code. Atomic coordinate files were deposited in the Protein Data Bank under the accession numbers PDB: 6V7U, PDB: 6V7V, PDB: 6V7W, and PDB: 6V7X.

EXPERIMENTAL MODEL AND SUBJECT DETAILS

Bacterial strains

E. coli and *P. aeruginosa* PA14 strains were routinely grown in lysogeny broth (LB) at 37°C with shaking or on LB agar plates at 37°C overnight. When required, antibiotics were added at the following concentrations: *E. coli*, ampicillin (100 μg/ml), kanamycin (50 μg/ml), or gentamicin (10 μg/ml); *P. aeruginosa* PA14, gentamicin (50 μg/ml). For protein expression in *P. aeruginosa,* the plasmid promoter was induced with 0.1% L-arabinose. In *E. coli* 1 mM isopropyl β-d-1-thiogalactopyranoside (IPTG) was used for protein expression.

Phage strains

Pseudomonas aeruginosa phages DMS3, DMS3vir and DMS3$^{\Delta aqs1}$ were propagated in PA14 and stored in SM buffer (100 mM NaCl, 8 mM Mg_2SO4, 50 mM Tris-HCl pH 7.5, 0.01% w/v gelatin) at 4°C.

METHOD DETAILS

DNA cloning and manipulation

A DMS3 lysogen was used for amplification of *aqs1* and *lasR* and lysogens of JBD24 and JBD26 were used for amplification of JBD24-*gp4* and *tip,* respectively. The genes were cloned into plasmids using Sequence and Ligation Independent cloning (SLIC) (Jeong et al., 2012) or restriction enzymes. For expression and protein purification in *E. coli*, *aqs1* was cloned into p15TV-L and pETDuet vectors. The bacterial-two hybrid assays had *aqs1* and targets cloned into either pUT18C or pKT25 vectors (Euromedex). Mutants were generated using a standard site-directed mutagenesis protocol. The desired mutation was generated via PCR with complementary primers encoding the mutated DNA sequence. PCR amplification was done with Phusion (Invitrogen) polymerase. The resulting PCR reaction was digested with *Dpn1*, transformed into *E. coli* DH5α and the plasmids containing the mutations were selected using the relevant antibiotic resistance and were sent for sequencing to confirm the mutation. All bacterial strains and oligonucleotides used in this study are summarized in the key resources table.

Pyocyanin production assay

For testing pyocyanin production in *Pseudomonas*, the wild-type and mutant Aqs1-expressing pHERD30T plasmids were transformed into *P. aeruginosa* strain PA14 and plated on LB agar containing 50 μg/ml gentamicin and incubated overnight at 37°C. The following day colonies were streaked out onto Pseudomonas isolation agar (PIA) supplemented with 50 μg/ml gentamicin, 0.1% arabinose, were incubated overnight at 37°C and production of the blue-green pyocyanin pigment was assessed visually after 24 hours incubation. Pyocyanin production was also monitored in 96-well plates. For this assay 2 μl of fresh overnight culture of the plasmid-expressed mutants or PA14$^{\Delta lasR}$ and PA14$^{\Delta pqsA}$ strains, were used to inoculate wells in a 96-well plate filled with 200 μl of Pseudomonas Isolation Agar (PIA) containing gentamicin and 0.1% L-arabinose. The production of pyocyanin was observed after 24 hours incubation at 37°C. Pyocyanin quantification from plates was performed as previously described (King et al., 2016); 2μl of overnight cultures were spotted onto PIA plates and the plates were incubated at 37°C for 24 hours. Samples of agar of 2 cm^2 were excised from the plate. Pyocyanin was extracted by the addition of 3 mL of chloroform, followed by second extraction with 0.2 N HCl, and the absorbance at 520 nm was measured. The OD_{520} of each sample was multiplied by the molar extinction coefficient of 17.072 to obtain the concentration of pyocyanin (μg/CFU).

Twitching motility assays

Twitching motility assays of *P. aeruginosa* PA14 expressing *aqs1* and various mutants were performed as previously described (Tsao et al., 2018). Briefly, individual colonies were stabbed through plates containing 1% LB supplemented with 50 μg/ml of gentamicin and 0.1% arabinose and incubated for 24 hours at 37°C. After incubation, the agar was carefully removed from the plates, and the

Please cite this article in press as: Shah et al., A phage-encoded anti-activator inhibits quorum sensing in *Pseudomonas aeruginosa*, Molecular Cell (2020), https://doi.org/10.1016/j.molcel.2020.12.011

biomass adhered to the bottom of the plates were stained with 1% crystal violet and washed with water. To determine the distance traveled by the bacteria, the diameter of the stained biomass was measured.

Protease production assay

PA14 transformed with empty vector or a plasmid expressing *aqs1* were grown overnight with shaking at 37°C in trypticase broth supplemented with 50 μg/mL gentamicin and 0.1% L-arabinose. The following morning cultures were equilibrated to OD_{600} 0.6 and 2 μL was spotted on top of trypticase soy agar agar plates supplemented with 20% skim milk, 50 mg of gentamycin and 0.1% L-arabinose. The plates were incubated 48 hours at 30°C. Protease production was assessed by the size of the zone of clearing surrounding the bacterial colony.

Rhamnolipid production assay

Cultures of PA14 transformed by empty vector or PA14 pHERD30T-*aqs1* were grown overnight with shaking at 37°C in trypticase soy broth supplemented with 50 μg/mL gentamicin and 0.1% L-arabinose. The following morning cultures were equilibrated to OD_{600} 0.6. To observe rhamnolipid production 5 μL of mineral oil was spotted on the lid of a polystyrene 96-well plate and equilibrated for an hour, after which 5 μL of equilibrated overnight culture was spotted onto the oil. The collapse of the culture drop, indicative of rhamnolipid production, was assessed after 1 minute.

Swarming motility assay

Swarming plates were made following the recipe Ha et al. (Ha et al., 2014). After autoclaving, M8 medium was supplemented with a final concentration of 0.2% glucose, 0.5% casamino acids, 1 mM $MgSO_4$, 50 μg/mL gentamicin and 0.2% L-arabinose. After pouring, the plates were dried for 30 minutes in a biosafety cabinet. They were then inoculated with 2.5 μL of overnight culture equilibrated to OD_{600} of 0.6 and were incubated at 37°C for 24 hours and the swarming zones were visually scored for distance traveled.

Identification of protein interaction partners using the bacterial two-hybrid assay

Bacterial-two hybrid analysis was performed as described previously (McCallum et al., 2016). *E. coli* BTH101 cells were co-transformed with the relevant pUT18C and pKT25 plasmid constructs and plated onto LB plates containing kanamycin, ampicillin, 1mM IPTG and 40 μg/ml X-gal. The plates were incubated at 30°C for two days and were examined for the presence of blue colonies, which indicates a positive interaction. Three independent colonies were picked from each plate and were grown overnight in LB containing antibiotics at 37°C with shaking. The following day the cultures were diluted 1/100 into fresh LB containing antibiotics and were grown to an OD_{600} of ~0.5. These cultures were used to quantify β-galactosidase activity and to inoculate MacConkey agar. Quantifying β-galactosidase activity was performed as follows, 50 μl of cultures was mixed with 50 μl of solution A (50 μL of 200 mm Na_2HPO_4, pH 7.4, 20 mm KCl, 2 mm $MgSO_4$, 0.8 mg/ml cetyltrimethylammonium bromide detergent, 0.4 mg/ml sodium deoxycholate, and 0.54% (v/v) β-mercaptoethanol) and 150μl of solution B (60 mm Na_2HPO_4, pH 7.4, 40 mm KCl, 1 mm ortho-nitrophenyl-β-galactoside, 20 μg/ml cetyltrimethylammonium bromide, 10 μg/ml sodium deoxycholate, and 0.27% (v/v) β-mercaptoethanol) and absorbance (A) measurements were taken at 420 nm and 550 nm every 5 minutes for 1 hour at 30°C in Synergy plate reader. β-galactosidase activity was calculated by finding the slope of $(A_{420} - 1.75 \times A_{550})$/(absorbance units × vol.) over time (min). For the MacConkey based plate assay, 2 μL of the cultures were spotted onto a MacConkey agar plate containing the appropriate antibiotics and 1 mM IPTG, and the plates were incubated at 30°C for 24 hours. Red pigmented colonies, which indicate acidification of the medium, were deemed positive interactions.

Protein expression and purification

L*asR* and *aqs1* were cloned into p15TV-L (GenBank accession EF456736), which contains a TEV cleavable N-terminal 6-His tag. For co-expression, genes were cloned into pETDuet (Novagen) with *lasR* in the MCS-1 site containing the N-terminal 6-His-tag and *aqs1* in the MCS-2 site (plasRFL-3-4_duet plasmid). Plasmids were transformed and propagated in *E. coli* MM294 cells in LB medium containing 100 μg/ml ampicillin. The SERp and methionine mutations in Aqs1 were created using site directed mutagenesis as described above. All plasmids were transformed into *E. coli* BL21(DE3) for protein expression and purification.

To obtain crystals of Aqs1, 20 mL of an overnight culture of cells expressing *aqs1* was used to inoculate 2L of LB containing 100 μg/ml ampicillin and the culture was grown at 37°C until the optical density (OD_{600}) reached 0.6-0.8. The culture was rapidly cooled to 20°C, induced with 1mM IPTG and incubated at 20°C overnight to allow protein expression. Cells were harvested by centrifugation and resuspended in cold binding buffer containing 20 mM Tris-HCl pH 7.5, 200 mM NaCl, and 5 mM imidazole. Cells were lysed by sonication and lysates were cleared by centrifugation for 20 minutes at 17000 rpm. The clarified lysate was incubated with 1 mL of Ni-NTA resin (QIAGEN) for 1 hour at 4°C. The resin was washed with 10 column volumes (CV) of wash buffer (binding buffer containing 30mM imidazole) before eluting the protein with elution buffer (binding buffer containing 300 mM imidazole). Eluted protein was mixed with 6-His tagged TEV protease and dialyzed overnight at 4°C in 20 mM Tris-HCl pH 7.5, 200 mM NaCl, 5 mM β-mercaptoethanol to allow cleavage of the 6-His-tag from Aqs1. The cleaved 6-His-tag and TEV protease were then removed by passing the protein solution over Ni-NTA resin. The purified Aqs1 protein was collected and concentrated to a final concentration of 20 mg/ml. The protein sample was further purified by size exclusion chromatography using a Hiload Superdex 75 16/600 column. Aqs1 ran as a single peak

Please cite this article in press as: Shah et al., A phage-encoded anti-activator inhibits quorum sensing in *Pseudomonas aeruginosa*, Molecular Cell (2020), https://doi.org/10.1016/j.molcel.2020.12.011

in 20 mM Tris-HCl, pH 7.5, 100 mM NaCl, which was used as the mobile phase buffer. Purity was assessed using SDS-PAGE and the recombinant protein was concentrated to 15 mg/ml and stored at 4°C.

Selenomethionine (Se-Met) labeled Aqs1 was prepared using the methionine auxotrophic *E. coli* BL21 (DE3) B834 strain cultured in M9 minimal medium containing 0.2% glucose and trace metals supplemented with Se-Met, and was purified using the same protocol as described above.

The expression and purification of LasR was carried out as described in (Kafle et al., 2016). For expression of LasR alone and in complex with Aqs1, the medium was supplemented with 20 μM 3-oxo-C_{12}-HSL (Sigma). The purification conditions used for the LasR-Aqs1 complex were same as that of LasR with the following modifications. After Ni-NTA purification, instead of ion-exchange chromatography the complex was concentrated to 20 mg/ml and was further purified by size-exclusion chromatography using Superdex S200 increase column. The single peak containing the LasR-Aqs1 complex was then concentrated to 15 mg/ml and used to set up crystal trays.

Crystallization of Aqs1 alone and LasR-Aqs1 complex

We were unable to get diffraction quality crystals of the full-length protein, so we used Surface Entropy Reduction (SERp) to enhance crystallization (Goldschmidt et al., 2007). Based on SERp server predictions we substituted two charged residues (Lys24, Glu25) with alanine. We also engineered methionine substitutions at two positions (Leu9, Leu22) to enable the structure to be determined using the single wavelength anomalous diffraction (Se-SAD) method. To ensure that these substitutions did not interfere with the activity of the protein, we examined both pyocyanin production and twitching motility in cells expressing this protein variant and confirmed they retained the phenotypes we observed upon expression of the wild-type protein (Figures S4A and S4B).

Purified full-length Aqs1 and the SERp mutant, as well as the LasR-Aqs1 complex, were initially screened with 1:1 (protein: precipitant) ratio against the MCSG commercial suite, Index and JCSG+ commercial screen using sitting drop vapor diffusion at 15 mg/ml. Full length Aqs1 protein did not crystallize in any of the conditions tested. Single crystals for the SERp mutant were observed in 1M NaH_2PO_4/K_2HPO_4, pH 5.0. The crystals were further optimized with 1:1 ratio sitting drop at 20°C in a precipitant condition composed of 1 M NaH_2PO_4/K_2HPO_4, pH 5.6 and 15% glycerol. Single crystals were also observed in a second condition that contained trisodium citrate, pH 5.5, 15% ethanol and 0.2M lithium sulfate. The crystals were further optimized with 1:1 ratio sitting drop at 20°C in a precipitant condition composed of 0.1 M tri-sodium citrate, pH 5.5, 15% ethanol, 0.2 M lithium sulfate and 15% glycerol. Single crystals for LasR-Aqs1 were observed in 0.2 M sodium chloride, 0.1 M HEPES:NaOH, pH 7.5 and 30% PEG400. Single crystals were also observed in another condition composed of 1.6 M ammonium sulfate, 0.1 M MES NAOH, pH 6.5 and 10% Dioxane. Crystals were cryoprotected in 15% glycerol.

Data collection and structure determination

$Aqs1^{SERpMet}$ mutant crystallographic data were collected on vitrified crystals at 105 K on 08ID-1 beam line at Canadian Light Source (CLS). Diffraction data from a total of 360 images were collected at wavelength 0.9795 using 1° oscillations. Data were processed with XDS (Kabsch, 2010) to a resolution of 2.5 Å. LasR-Aqs1 complex crystallographic data were collected at NECAT beamline 24-ID-C at the Advanced Photon Source (APS, Chicago, USA). The Aqs1 structure was solved using selenium single wavelength anomalous dispersion (Se-SAD). This structure was then used as a molecular replacement (MR) search model for the solution of the LasR-Aqs1 complex. Additionally, the LasR ligand-binding domain bound to AHL (PDB 3IX3) was used as an independent search model for MR. All MR and automated refinement were performed with the PHENIX suite (Liebschner et al., 2019). Manual refinement was undertaken with Coot (Emsley et al., 2010). PyMol was used for molecular modeling and graphics (Schrodinger, 2015). Atomic coordinate files were deposited in the Protein Data Bank under the accession numbers 6V7U, 6V7V, 6V7W, and 6V7X.

Size exclusion chromatography-multi angle light scattering (SEC-MALS)

Light scattering measurements for Aqs1 were performed using a Malvern Viscotek GPCmax system connected to a Superdex 75 gel filtration column (GE Healthcare). Samples were applied in a volume of 150 μL to a column equilibrated in 20 mM Tris-HCl, pH 8.0, and 100 mM NaCl at a flow rate of 0.5 ml/minutes. The scattered light intensity of the column eluate was recorded using VE 3580 RI and Malvern 270 Dual detector. Bovine serum albumin at a concentration of 1 mg/ml was used for detector normalization. Molecular weights were calculated from Zimm plots using a protein refractive index increment, dn/dc, of 0.185 mL/g using the OmniSEC 5.10 software (Malvern).

Electrophoretic mobility shift assays (EMSAs)

EMSAs were performed as described in Kafle et al. (Sandoz et al., 2007). Briefly, binding reactions were performed in binding buffer containing 0.7 mm KH_2PO_4, 2.15 mm Na_2HPO_4, 1.35 mm KCl, 20 mm NaCl, 0.5 mm EDTA, 0.05% (v/v) Triton X-100 and 5% (v/v) glycerol. A 43-mer DNA duplex containing the *lasB* OP1 site (5′-ATCAAGGCTACCTGCCAGTTCTGGCAGGTTTGGCCGCG GGTTC-3′) annealed to its complementary strand with 5′ modification of the top strand with fluorescein (6-FAM, Integrated DNA Technologies) was used for all binding assays. For binding assays, purified proteins were incubated with 100 nM *lasB* OP1 site for 30 minutes at 25°C before separation on a 6% nondenaturing polyacrylamide gel with 0.5X Tris borate-EDTA as the running buffer. To determine if Aqs1 could displace bound DNA, 15μM LasR was incubated with *lasB* OP1 for 30 minutes, then 15μM Aqs1 was added and incubated for 30 minutes before electrophoresis.

Please cite this article in press as: Shah et al., A phage-encoded anti-activator inhibits quorum sensing in *Pseudomonas aeruginosa*, Molecular Cell (2020), https://doi.org/10.1016/j.molcel.2020.12.011

Preparation of P. aeruginosa phages and plaque assays

P. aeruginosa lysogens were grown overnight in LB medium at 37°C for phage propagation through spontaneous induction. To isolate phages from the culture, the bacterial cells from the overnight culture were lysed by the addition of a few drops of chloroform and subsequent shaking at 37°C for 30 minutes. Cellular debris was collected by centrifugation at 15000 x g for 10 minutes. The phage lysate was stored at 4°C with a few drops of chloroform to keep it sterile.

To assess the sensitivity of bacteria to various phages, serial dilutions of phages were spotted onto lawns of bacteria in the plaquing assay. To create a lawn of bacteria, 150 μL of overnight bacterial culture was added to 3 mL of 0.7% molten top agar and poured atop 1.5% LB agar plates. Both the top agar and bottom plate were supplemented with 10 mM $MgSO_4$ and 50 μg/ml of gentamicin and 0.1% L-arabinose where required. 2 μL of 10-fold serial dilutions of phages were spotted onto the bacterial lawns, and the plates were incubated at 30°C overnight.

Generating mutants of aqs1 in the DMS3 phage

We created a recombination cassette for the *aqs1* deletion mutant by amplifying *dms3-2* and *dms3-4* along with flanking regions that contain homology to the 5′ and 3′ regions of *aqs1*. The primers were designed to make an in-frame deletion of *aqs1* while maintaining a short sequence from the 5′ and 3′ regions to prevent polarity effects (see Table S2 for primers). This cassette was cloned into pHERD30T and transformed into the PA14 DMS3 lysogen. Phages were isolated after overnight growth and a plaque assay was performed by infecting 150 μL of PA14 empty vector or PA14 expressing pHERD30T-Cas9 containing guide RNA spanning nucleotides 97 to 117 of *aqs1*, with 10 μl overnight phage. For optimum killing of wild-type phages the pHERD30T-Cas9 construct was grown overnight in the presence of 50 μg/ml gentamicin and induced with 0.1% L-arabinose. After a 10 minute incubation the culture was added to 3 mL of top agar and poured onto a thick LB agar plate supplemented with 10 mM MgSO4, 50 ug/ml gentamicin and 0.1% L-arabinose, and was incubated overnight at 30°C. Phages that acquired the *aqs1* deletion were capable of forming isolated plaques on the lawn of PA14 expressing Cas9 targeting *aqs1*. Individual plaques were resuspended in LB and 2 μl of ten-fold serial dilutions of these samples were spotted onto a fresh lawn of PA14-pHERD30T-Cas9 and incubated overnight at 30°C. The following day, newly generated plaques were resuspended in LB. To confirm the deletion, a Phusion (Invitrogen) PCR reaction was performed with the various phage isolates and WT DMS3 as a control with primers specific to *dms3-2* and *dms3-4*. Phage isolates with an observed product smaller than WT were sent for sequencing to confirm the deletion.

PA14 phage infection assays

Overnight cultures of PA14 or the indicated knockout strain were diluted 1/100 into fresh LB medium containing 10 mM $MgSO_4$ and 150 μl was dispensed into the wells of a clear 96-well plate. Cell were immediately mixed with phages, DMS3 and DMS3$^{\Delta aqs1}$, respectively at a multiplicity of infection (MOI) of 10, 1, 0.1, 0.01, and 0.001 and were grown at 37°C with shaking in an Infinity TECAN microplate reader. Cell density was monitored using the associated Magellan™ software package. Cell growth was monitored by measuring the OD_{600} every 30 minutes for 14-hours. Each cell and phage combination was tested at least three times.

P. aeruginosa PA14 cell counts and lysogen determination during phage infection

PA14 overnight cultures were diluted 1/100 in two separate tubes containing 5 mL of fresh LB supplemented with 10 mM $MgSO_4$. To perform the assay, DMS3 and DMS3$^{\Delta aqs1}$ were added to the fresh PA14 dilutions at an MOI of 1 and 150 μL of the cell-phage mixtures were dispensed into the wells of a 96 well plate. These cultures were grown at 37°C with shaking in a TECAN microplate reader and the OD_{600} was monitored. To determine cell and phage counts at the various time points, a 150 μl sample was centrifuged at 21,000 x g for 1 minute, the supernatant was removed and was saved for phage enumeration as outlined below. The cell pellet was resuspended in 150 mL of fresh LB, the cells were collected by centrifugation again to wash away any contaminating phages, and then were resuspended in 150 μL of LB. Ten-fold serial dilutions were performed, the cells were plated on LB agar and grown overnight at 37°C. The following day the colonies were counted. To determine the number of phages at each time point the supernatant was put into a fresh tube containing chloroform and was vortexed for ten seconds. Ten-fold serial dilutions of the phage samples were prepared and 2 μl aliquots were spotted onto lawns of PA14 and incubated overnight at 30°C. The following day the number of plaque forming units (pfu) was determined. To determine the number of lysogens formed, 52 colonies were selected from each time point of the DMS3 or DMS3$^{\Delta aqs1}$growth assay plates, point inoculated onto a lawn of PA14 seeded in top agar, and were grown overnight at 30°C. A zone of clearing around the inoculation site signified spontaneous phage production and indicated which colonies were lysogens.

Spontaneous phage induction in liquid culture growth measurement

To determine the amount of phage spontaneously produced by wild-type and mutant DMS3 lysogens, 1 mL of cells from overnight cultures were collected by centrifugation and resuspended in fresh medium three times before a final dilution to 1/100 in 20 mL of LB supplemented with 10 mM $MgSO_4$. Cells were grown at 37°C with shaking in a flask and the OD_{600} was measured every hour until approximately 6 hours or the onset of visible pyocyanin production. Each hour, 500 μL of cells were collected by centrifugation, the supernatant was treated with chloroform and serial dilutions of the phage-containing supernatant were spotted on a lawn of PA14. These cultures were incubated overnight at 30°C before the number of plaques was determined.

Please cite this article in press as: Shah et al., A phage-encoded anti-activator inhibits quorum sensing in *Pseudomonas aeruginosa*, Molecular Cell (2020), https://doi.org/10.1016/j.molcel.2020.12.011

PQS quantification during infection with phage DMS3

An overnight culture of PA14 was diluted 1/100 in LB medium supplemented with 10 mM $MgSO_4$ and was separated into three samples: cells alone, PA14 infected with DMS3, and PA14 infected with DMS3$^{\Delta aqs1}$. 200 μL of the cultures were dispensed into the wells of a 96-well plate and were grown with shaking at 37°C. At five hours post infection the samples for each group were pooled and cells and debris were collected by centrifugation for 1 minute at 21,000 x g. The supernatants were filtered through a 0.2 μM filter and stored at −20°C.

One mL of cell-free supernatant was mixed with 750 μL of acidified ethyl acetate (0.01% glacial acetic acid) and mixed by vortexing for 30 s. The samples were separated by centrifugation at 15,000 rpm for 1 minute and the ethyl acetate (top) layer was transferred to a fresh microfuge tube. This extraction procedure was repeated and the samples were transferred to a 16x100mm glass tube and placed in the Genevac on the low BP program (1.2 hours). 100 μL of acetonitrile (LC-MS grade) was added to each sample, followed by sonication for 30 s with gentle swirling. The samples were then transferred to a fresh microfuge tube and were centrifuged at 15,000 rpm for 3 minutes. 50 μL of the resulting supernatant was transferred to a sample vial with insert.

Quantification of PQS was performed by LC-MS/MS using a Waters Alliance I-Class coupled to Xevo G2-S QToF. 5 μL of each sample was injected into an Acquity UPLC BEH C18 column (2.1x50mm, 1.7 μM) at 40°C. A flow rate of 0.2 mL/minute was used. The solvents used were A = H_2O+0.1% FA; B = MeCN+0.1% FS with the following protocol: 20%B – 50%B (1-2 min.), 50%B – 95% B (2-5 min.), 95%B (5-7 min.), 95%B – 20%B (7-8 min.), 20%B (8-10 min.).

RNA Extraction and RT-qPCR of DMS3 during infection

Overnight cultures of PA14 were subcultured 1:100 in LB medium and were grown at 37°C with shaking to OD_{600} of 0.4. One mL of culture was removed as an uninfected control before the addition of phage DMS3vir, a virulent mutant of DMS3 that is unable to form lysogens (Cady et al., 2012), at an MOI of 10. The culture was incubated at 37°C with shaking while samples were removed, harvested by centrifugation and flash frozen 0, 10 and 60 minutes post phage addition. Cells were harvested following the 10-minute time point and resuspended into fresh pre-warmed LB to decrease the possibility that multiple rounds of infection would occur.

Frozen cell pellets were resuspended in 800 μL LB and mixed with 100 μL lysis buffer (40 mM sodium acetate, 1% SDS, 16 mM EDTA) and 700 μL acid phenol:chloroform, pH 4.5 (Ambion) pre-heated to 65°C. The mixture was incubated at 65°C for 5 minutes with regular vortexing and centrifuged at 12,000 x g for 10 minutes at 4°C. The aqueous layer was collected, extracted with chloroform, and precipitated with ethanol. Total RNA extracts were treated with DNase (TURBO DNA-free kit, Ambion) according to the manufacturer's instructions. cDNA was synthesized from 1 μg of DNA-free RNA using SuperScript IV VILO master mix (Invitrogen) and quantified using PowerUp SYBR green master mix (Applied Biosystems) with primers listed in Table S2. For the purpose of quantification, standards were generated by PCR. Data were analyzed using BioRad CFX Maestro software.

QUANTIFICATION AND STATISTICAL ANALYSIS

All experiments were performed with at least three biological replicates ($n \geq 3$). Statistical parameters are reported in the Figure Legends.